Atmospheric Pollution Research 2 (2011) 318-336

Atmospheric Pollution Research

www.atmospolres.com

Source apportionment of fine particulate matter over the Eastern U.S. Part II: source apportionment simulations using CAMx/PSAT and comparisons with CMAQ source sensitivity simulations

Michael J. Burr, Yang Zhang

Department of Marine, Earth, and Atmospheric Sciences, North Carolina State University, Raleigh, NC, 27695, USA

ABSTRACT

This Part II paper describes source apportionment (SA) for 10 source categories at a 12 km horizontal grid resolution over the eastern U.S. for January and July of 2002 using the Comprehensive Air Quality Model with extensions/Particulate Source Apportionment Technology (CAMx/PSAT). SA results from CAMx/PSAT are contrasted with those from CMAQ/BFM in Part I. The top three sources domainwide in January are identified to be coal combustion (with a monthly–mean contribution of 14.0%, or 1.1 μg m^{-3}), biomass burning (11.3%, 0.9 μg m^{-3}) and other mobile sources (6.8%, 0.6 μg m^{-3}) by CAMx/PSAT but biomass burning (13.7%, 1.1 μg m^{-3}), miscellaneous area sources (11.8%, 0.9 μg m^{-3}), and coal combustion (10.8%, 0.9 μg m^{-3}) by CMAQ/BFM. Both agree that coal combustion, industrial processes, and miscellaneous area sources are the top three sources in July, though they differ in the magnitude of contributions. Both give similar contributions for primary PM, but they differ substantially in SA results for secondary PM, due primarily to their treatments for oxidant–limiting and indirect effects. While CMAQ/BFM inherently accounts for these effects and can provide useful information for primary and secondary PM species, CAMx/PSAT neglects them by linking each PM species only with its direct primary emission precursor. These effects are enhanced in January due to the increased importance of NO_3^- and lower concentrations of oxidants relative to July. CAMx/PSAT is thus accurate for SA of the primary PM species but incorrect in its SA for secondary PM species. For a highly non–linear system studied here, the true SA cannot be obtained with current SA methods. Policy–makers must be mindful of relative strengths and weaknesses of each method, as well as the limitation of current SA methods in the SA of secondary PM species, when using such information in support of state implementation plan and epidemiological studies.

Keywords:
$PM_{2.5}$
Particulate source apportionment technology
Brute–Force source sensitivity method
CMAQ
CAMx
Southeastern U.S.

Article History:
Received: 26 September 2010
Revised: 14 January 2011
Accepted: 23 January 2011

Corresponding Author:
Yang Zhang
Tel: +1-919-515-9688
Fax: +1-919-515-7802
E–mail: yang_zhang@ncsu.edu

doi: 10.5094/APR.2011.037

1. Introduction

Quantifying the contributions of various emission sources to ambient $PM_{2.5}$ concentrations is an important first step in developing the most effective control strategies. As described in Burr and Zhang (2011), the source sensitivity (SS) and the source apportionment (SA) are two different source–oriented methods that are commonly used to determine source–receptor relationships for particulate matter with an aerodynamic diameter of less than 2.5 microns ($PM_{2.5}$). Each method has its own strengths and weaknesses. While there have been studies comparing SS and SA for ozone (e.g., Dunker et al., 2002; Cohan et al., 2005; Zhang et al., 2005), comparisons of these methods for PM are limited. Baek et al. (2005) compared the brute–force method (BFM) with a reactive tracers method within the Community Multiscale Air Quality (CMAQ) modeling system (referred to as CMAQ/BFM and CMAQ–TR, respectively) for primary organic aerosols and found that the two methods gave nearly identical contributions from all source categories as expected for primary species. Koo et al. (2009) compared the Particulate Source Apportionment Technology (PSAT) and the Brute Force Method (BFM) within the Comprehensive Air Quality model with Extensions (CAMx) (referred to as CAMx/PSAT and CAMx/BFM, respectively) for PM for SO_2 and NO_x emissions from point sources, NO_x, VOC, and NH_3 emissions from area sources, and all emission species from on–road mobile sources. They found that the source contributions by CAMx/PSAT and CAMx/BFM are equivalent for primary aerosol species and similar in situations where the indirect effect is insignificant. Contrasting with the direct effects in which the concentrations of a PM species (e.g., NH_4^+) respond to changes in the emissions of its direct precursor (e.g., NH_3), such indirect effects result from interactions between secondary PM species and non–direct gaseous precursors (e.g., NH_4^+ concentrations vary with changes in SO_2 emissions). However, as the indirect effects become more important, the SA results from CAMx/PSAT and CAMx/BFM deviate.

Following the Part I that describes SS results from CMAQ/BFM (Burr and Zhang, 2011), this Part II paper describes the SA results from CAMx/PSAT and compares them with those of CMAQ/BFM.

While other studies have primarily considered emissions of a single species from limited source categories (< 5), this study provides a comprehensive comparison of CAMx/PSAT and CMAQ/BFM for all emission species from 10 major source categories. Detailed explanations for the large differences between the two methods are given along with a discussion on the applicability of each method based on their respective strengths and limitations.

2. Model Configurations and Simulation Design

CAMx version 5.00 with the PSAT is used to conduct source apportionment for the same 10 source categories as those summarized in Table S2 of Part I paper of Burr and Zhang (2011) over the eastern U.S. at a 12 km horizontal grid resolution in January and July of 2002. All inputs for chemistry and meteorology are identical to those used for CMAQ/BFM in Part I paper. While both models use meteorology simulated from MM5, CAMx uses the MM5CAMx processor to prepare meteorological fields for use within CAMx. This may cause some differences in the meteorological fields between the two models, as some variables (e.g., wind fields and cloud fractions) are recalculated in the meteorological processors. Similarly, the CMAQ2CAMx processor is used to generate CAMx ready model emissions based on emissions files processed from SMOKE.

Table 1 compares the model configurations used in both models. The model configurations in CAMx/PSAT are selected to be similar to CMAQ wherever possible in order to minimize differences between baseline simulations using both models. Several differences, however, remain. These include differences in secondary organic aerosol (SOA) modules, vertical mixing schemes, wet and dry deposition modules, and PM size representations; such differences will contribute partially to differences in the baseline simulations of CMAQ and CAMx, and thus in the SA results from CMAQ/BFM and CAMx/PSAT.

Similar to CMAQ/BFM, the baseline simulation from CAMx is first evaluated using observations from various networks in terms of monthly–average max 8–h average O_3 mixing ratios and concentrations of $PM_{2.5}$ and its individual species (i.e. $PM_{2.5}$, ammonium (NH_4^+), sulfate (SO_4^{2-}), nitrate (NO_3^-), black carbon (BC), organic carbon (OC), and total carbon (TC = BC + OC). Monthly–mean contributions of each source to the concentrations of $PM_{2.5}$ and its components from CAMx/PSAT are then analyzed as absolute and percentage contributions of each source with respect to the total $PM_{2.5}$ concentrations. These results are compared with those obtained from CMAQ/BFM in Part I (Burr and Zhang, 2011). The major differences between the SA results using the two methods along with possible factors causing such differences are examined. Additionally, results obtained from CAMx/PSAT and CMAQ/BFM are compared with receptor–based methods from previous studies.

3. Evaluation of Surface Predictions of CAMx

Table 2, Table S1, and Table S2 (see the Supporting Material, SM) summarize the performance statistics for surface concentrations of max 1–hr and 8–hr O_3 as well as 24–h average $PM_{2.5}$ and its individual species from CAMx. These results are discussed and compared with those from CMAQ as shown in Tables 2, S2, and S3 in Part I. Max 1–h and 8–h O_3 mixing ratios are overpredicted by both models at all sites in January with the exception of the SEARCH sites, where CMAQ slightly underpredicts. CAMx gives higher concentrations than CMAQ for both max 1– and 8–h average O_3 at all sites. This may be due to a weaker vertical mixing within CAMx as a result of the use of different vertical mixing schemes as described in Olsen (2009). The weaker vertical mixing may also influence $PM_{2.5}$ formation, as CAMx generally gives higher $PM_{2.5}$, though both models overpredict in January at all sites. For the same reason, CAMx gives higher concentrations of all carbon species (TC, BC, and OC) at all sites in January. Differences in simulated concentrations of certain oxidant and radical species may also affect the differences in simulated OC between CAMx and CMAQ. For example, higher O_3 concentrations by CAMx can lead to higher oxidation of VOCs, ultimately leading to more simulated SOA in both months. Additional processes such as parameters for heterogeneous reactions, dry and wet deposition and/or PM size representations may also be important. For example, in January, CMAQ overpredicts NO_3^- concentrations while CAMx underpredicts them at all sites, with the exception of SEARCH sites which show a slight overprediction. This may be partially explained by differences in the uptake coefficient (γ) used for the heterogeneous reaction of N_2O_5 between CMAQ and CAMx. The upper and lower bounds of γ are 0.02 and 0.002 in CMAQ and 0.017 and 0.001 in CAMx, respectively. The slightly larger γ values in CMAQ may partially explain the higher prediction of NO_3^- from CMAQ in January. Conversely, CMAQ tends to underpredict SO_4^{2-} concentrations at all networks with the exception of SEARCH, while CAMx overpredicts them at SEARCH, IMPROVE, and AIRS–AQS sites. This is due mainly to differences in wet deposition between the two models, with CMAQ giving higher wet deposition fluxes of SO_4^{2-} in January than CAMx (see the SM, Figure S1). Large values for MNE and MNB (100 – 300%) occur for similar species at similar sites for both CMAQ and CAMx (e.g., SO_4^{2-}, NO_3^-, NH_4^+, BC, and TC at SEARCH sites, NH_4^+ at STN sites). These inflated values are caused by increasingly small hourly observations occurring at these sites.

In July, CAMx tends to overpredict both max 1– and 8–h average O_3 mixing ratios with normalized mean biases (NMBs) of 7.9–31.4% while CMAQ underpredicts with NMBs of –0.7% to –7.4%, due to its weaker vertical mixing. With the exception of SO_4^{2-} at the SEARCH sites from CMAQ and CAMx , SO_4^{2-} at the IMPROVE and CASTNET sites from CAMx, and BC at the SEARCH sites from CAMx, concentrations of all $PM_{2.5}$ components are underpredicted by both models in July. This underprediction may be due to uncertainties in model inputs (e.g., emissions of gaseous PM precursors such as NO_x and VOCs) and biases in meteorological predictions (e.g., precipitation and vertical mixing). The spatial distributions of CAMx predictions for 24–h average $PM_{2.5}$ and max 8–hr O_3 along with analysis are given in the mode evaluation section of the SM. Large values for MNB and MNE again occur for SO_4^{2-}, NO_3^-, and BC at SEARCH sites for both CMAQ and CAMx, caused by small hourly observations at these sites.

Table 1. *CMAQ and CAMx configurations used in this work (Olsen, 2009)*

	CMAQ v4.51	**CAMx v5.00**
Horizontal Advection	Yamartino–Blackman Cubic	PPM
Horizontal Diffusion	Explicit	Explicit
Vertical Advection	Yamartino–Blackman Cubic	Implicit
Vertical Diffusion	Semi–Implicit K–theory	Implicit
Gas–Phase Chemistry	CB–IV	CB–IV
Aqueous Phase Chemistry	RADM	RADM
PM Size Representation	Modal (i.e., nuclei, accumulation, coarse)	Sectional (2 bins)
Inorganic Aerosol Thermodynamics	ISORROPIA v1.5	ISORROPIA v1.6
Secondary Organic Aerosols	SORGAM	SOAP
Dry Deposition	M3DRY	Wesley (1989)
Wet Deposition	Accumulation and coarse mode particles absorbed in water; nuclei mode slowly scavenged; Henry's law for gases	All PM assumed in cloud water; Henry's law for gases

PPM: Piecewise Parabolic Method; CB–IV: Carbon Bond IV; RADM: Regional Acid Deposition Model;
SORGAM: Secondary Organic Aerosol Model; SOAP: Secondary Organic Aerosol Partitioning; M3DRY: Models–3 Dry Deposition Module

Table 2. *Performance statistics for surface concentrations simulated by CAMx in January and July 2002*

January										
Variable	**Network**	**MeanObs**	**MeanSim**	**Number**	**NMB**	**NME**	**MNB**	**MNE**	**RMSE**	**COR**
Max 1-h O_3	AIRS-AQS	31.3	35.4	6 191	12.5	24.3	19.3	31.2	9.6	72.3
	CASTNET	33.4	36.2	1 321	8.6	20.3	10.3	22.9	8.6	68.4
	SEARCH	34.4	35.0	62	1.9	20.7	4.5	23.1	8.9	65.1
Max 8-h O_3	AIRS-AQS	26.3	30.7	6 189	15.2	27.4	23.8	37.2	9.2	73.7
	CASTNET	30.1	33.5	1 317	11.6	23.1	15.1	26.8	8.8	66.4
	SEARCH	27.7	29.3	61	6.5	23.6	9.4	25.7	7.9	76.4
24-h avg. $PM_{2.5}$	IMPROVE	7.7	9.3	292	21.6	36.4	31.4	43.2	3.9	68.7
	SEARCH	10.2	16.6	1 218	63.1	83.8	78.1	90.3	12.1	34.3
	STN	12.9	16.7	518	29.5	49.5	40.6	56.9	9.9	46.9
	AIRS-AQS	13.0	14.5	8 489	12.6	37.8	19.3	41.2	7.7	51.3
July										
Variable	**Network**	**MeanObs**	**MeanSim**	**Number**	**NMB**	**NME**	**MNB**	**MNE**	**RMSE**	**COR**
Max 1-h O_3	AIRS-AQS	65.1	72.9	20 306	12.6	22.4	19.3	25.8	18.6	66.3
	CASTNET	64.1	68.6	1 349	7.9	18.2	12.3	19.8	14.5	67.3
	SEARCH	73.9	88.7	60	20.2	23.1	23.1	25.4	22.2	69.5
Max 8-h O_3	AIRS-AQS	57.0	66.8	20 297	17.6	24.2	25.6	30.7	17.7	68.4
	CASTNET	57.2	64.6	1341	13.2	20.4	18.7	24.6	14.8	67.5
	SEARCH	60.3	79.2	57	31.4	32.7	44.3	43.9	24.0	64.6
24-h avg. $PM_{2.5}$	IMPROVE	17.4	10.8	342	-37.8	47.2	-26.3	51.4	11.2	59.3
	SEARCH	19.7	15.8	1 203	-19.8	47.3	5.2	59.4	12.6	33.1
	STN	21.0	15.0	806	-28.5	48.1	Inf	Inf	14.6	45.8
	AIRS-AQS	20.2	14.2	8 386	-29.8	44.3	Inf	Inf	12.5	54.2

MeanObs: Mean Observed Values (ppb for O_3, μg m^{-3} for $PM_{2.5}$); MeanSim: Mean Simulated Values (ppb for O_3, μg m^{-3} for $PM_{2.5}$); NMB: Normalized Mean Bias; NME: Normalized Mean Error, MNB: Mean Normalized Bias; MNE: Mean Normalized Error; RMSE: Root Mean Square Error; COR: Correlation Coefficient; Inf: Infinity

4. Comparison of CAMx/PSAT and CMAQ/BFM Source Contributions

4.1. Monthly–mean domainwide source contributions

Tables 3 and 4 show the domainwide monthly–mean percentage contributions of each source category to $PM_{2.5}$ and its individual species in January and July, respectively. The corresponding monthly–mean absolute contributions are given in Tables 5 and 6. In January, coal combustion contributes the greatest to domainwide $PM_{2.5}$, with a monthly–mean contribution of 14% (1.1 μg m^{-3}). Among all PM species, coal combustion contributes the most to SO_4^{2-} (11.4% (0.9 μg m^{-3}) of the overall contribution of coal combustion to $PM_{2.5}$). Biomass burning and other mobile sources are the other two top source categories with monthly–mean domainwide contributions of 11.3% (0.9 μg m^{-3}) and 6.8% (0.6 μg m^{-3}), respectively. In July, coal combustion is the dominant source category, contributing to nearly 21% (1.6 μg m^{-3}) of domainwide monthly–mean $PM_{2.5}$, with SO_4^{2-} accounting for approximately 20.2% (1.6 μg m^{-3}) of the overall contribution. Miscellaneous area sources and industrial processes are the other two top source categories with monthly–mean domainwide contributions of 8.1% (0.6 μg m^{-3}) and 6.2% (0.5 μg m^{-3}), respectively. Approximately 5% (0.2 μg m^{-3}) and 10% (0.6 μg m^{-3}) of the monthly–mean $PM_{2.5}$ is not accounted for within the 12 source categories (including initial and boundary conditions) in January and July, respectively. This may indicate the influence of the source categories not examined in the application of CAMx/PSAT (e.g., aircraft, offshore/shipping, and Canadian point sources). As previously mentioned, the contributions of both initial and boundary conditions are tracked separately within CAMx/PSAT. Within CAMx/PSAT, boundary conditions contributed ~30% (2.4 μg m^{-3}) and ~27% (2.1 μg m^{-3}) of monthly–mean $PM_{2.5}$ in January and July, respectively. These relatively large contributions from boundary conditions indicate the impacts of long–range transport of pollutants from outside the domain. Additionally, initial conditions contribute ~4% (0.3 μg m^{-3}) and ~5% (0.4 μg m^{-3}) of monthly–mean $PM_{2.5}$ in January and July, respectively.

In January, CAMx/PSAT and CMAQ/BFM give different SA results in terms of both magnitude and overall rankings. The top three source categories (in order from 1st to 3rd) are biomass burning, miscellaneous area sources, and coal combustion by CMAQ/BFM and coal combustion, biomass burning, and other mobile sources by CAMx/PSAT. In July, the results from the two methods are more comparable overall, with coal combustion, industrial processes, and miscellaneous area sources as the top three source categories. However, there are fairly large discrepancies between CMAQ/BFM and CAMx/PSAT in the contributions of coal combustion [~31% (2.3 μg m^{-3}) vs. ~21% (1.6 μg m^{-3})] and biogenic contributions [1.5% (0.1 μg m^{-3}) vs. 4.5% (0.4 μg m^{-3})] in July, which will be explained by spatial distributions of the source contributions in the following Section. Both models agree that diesel vehicles and waste disposal and treatment are two relatively insignificant source categories in January, with contributions of < 3%. Similarly, both models agree that diesel vehicles, gasoline vehicles, and waste disposal and treatment have small contributions (< 3%) in July.

4.2. Spatial distributions of CAMx/PSAT source contributions

Figures 1 and 2 show the monthly–mean percentage contributions of each source category to $PM_{2.5}$ concentrations in January and July, respectively, as resolved by CAMx/PSAT. Additionally, Figures 3 and 4 show the contributions to the concentrations of SO_4^{2-}, NO_3^-, POA, and SOA from the top 3 source categories in January and July, respectively. Similar plots are shown for CMAQ/BFM in Figures 1, 2, 4, and 5 in Part I (Burr and Zhang, 2011).

In January, biomass burning contributions to $PM_{2.5}$ from CAMx/PSAT and CMAQ/BFM are fairly similar both spatially and in magnitude. As shown in Tables 3 and 4, biomass burning contributions are dominated by primary species (e.g., POA and OIN) in both months. Both methods give similar contributions to primary species whose concentrations are linearly related to emissions, with some slight differences due to differences (i.e., dry and wet deposition) in the underlying host models. CMAQ/BFM also agree well on the contributions to $PM_{2.5}$ from industrial processes, other mobile sources, and waste disposal and treatment in January due to the dominance of primary PM species in the

Table 3. *Domainwide monthly-mean percentage contributions to the concentrations of $PM_{2.5}$ and its components in January from CAMx/PSAT*

Source	NH_4^+	SO_4^{2-}	NO_3^-	EC	POA	SOA	OIN	$PM_{2.5}$
Coal Combustion	0.02	11.39	1.32	0.03	0.02	0.00	1.21	13.99
Diesel Vehicles	0.04	0.28	1.19	0.90	0.37	0.00	0.02	2.80
Biomass Burning	0.29	0.31	0.08	1.17	6.36	0.06	3.03	11.30
Gasoline Vehicles	1.20	0.28	1.46	0.06	0.26	0.06	0.17	3.49
Industrial Processes	0.68	2.05	0.25	0.04	0.70	0.08	2.49	6.29
Waste Disposal and Treatment	0.05	0.02	0.01	0.02	0.21	0.00	0.18	0.49
Biogenic	0.30	0.00	0.15	0.00	0.01	1.87	0.11	2.44
Other Combustion	0.14	2.31	0.83	0.26	1.83	0.01	1.11	6.49
Other Mobile	0.00	0.13	0.43	0.22	0.69	0.03	5.28	6.78
Miscellaneous Area Sources	4.61	0.00	0.00	0.00	0.02	0.00	0.35	4.98
Initial Conditions	0.46	1.41	0.68	0.13	0.45	0.03	0.76	3.92
Boundary Conditions	2.85	15.07	3.77	0.84	3.05	0.13	4.24	29.95
Sum	10.64	33.25	10.17	3.67	13.97	2.27	18.95	92.92

EC: Elemental Carbon; POA: Primary Organic Aerosol; SOA: Secondary Organic Aerosol; OIN: Other Inorganics

Table 4. *Domainwide monthly-mean percentage contributions to the concentrations of $PM_{2.5}$ and its components in July from CAMx/PSAT*

Source	NH_4^+	SO_4^{2-}	NO_3^-	EC	POA	SOA	OIN	$PM_{2.5}$
Coal Combustion	0.01	20.24	0.06	0.01	0.01	0.00	0.66	20.99
Diesel Vehicles	0.02	0.55	0.10	1.10	0.40	0.00	0.02	2.19
Biomass Burning	0.07	0.19	0.00	0.25	1.33	0.00	0.82	2.66
Gasoline Vehicles	0.79	0.38	0.07	0.05	0.29	0.03	0.15	1.76
Industrial Processes	0.33	2.58	0.02	0.03	0.52	0.03	2.68	6.19
Waste Disposal and Treatment	0.04	0.04	0.00	0.01	0.15	0.00	0.13	0.37
Biogenic	0.19	0.00	0.05	0.00	0.00	4.22	0.07	4.53
Other Combustion	0.05	3.25	0.04	0.05	0.48	0.00	0.30	4.17
Other Mobile	0.00	0.39	0.04	0.33	0.57	0.01	4.17	5.51
Miscellaneous Area Sources	5.57	0.00	0.00	0.01	0.14	0.00	2.39	8.11
Initial Conditions	0.44	3.84	0.01	0.10	0.32	0.04	0.36	5.11
Boundary Conditions	2.39	15.80	0.05	1.36	5.16	0.12	1.82	26.70
Sum	9.9	47.26	0.44	3.3	9.37	4.45	13.57	88.29

EC: Elemental Carbon; POA: Primary Organic Aerosol; SOA: Secondary Organic Aerosol; OIN: Other Inorganics.

Table 5. *Domainwide monthly-mean absolute ($\mu g\ m^{-3}$) contributions to the concentrations of $PM_{2.5}$ and its components in January from CAMx/PSAT*

Source	NH_4^+	SO_4^{2-}	NO_3^-	EC	POA	SOA	OIN	$PM_{2.5}$
Coal Combustion	0.00	0.92	0.11	0.00	0.00	0.00	0.10	1.12
Diesel Vehicles	0.00	0.02	0.10	0.07	0.03	0.00	0.00	0.23
Biomass Burning	0.02	0.02	0.01	0.09	0.51	0.00	0.24	0.91
Gasoline Vehicles	0.10	0.02	0.12	0.00	0.02	0.00	0.01	0.28
Industrial Processes	0.05	0.16	0.02	0.00	0.06	0.01	0.20	0.51
Waste Disposal and Treatment	0.00	0.00	0.00	0.00	0.02	0.00	0.01	0.04
Biogenic	0.02	0.00	0.01	0.00	0.00	0.15	0.01	0.20
Other Combustion	0.01	0.19	0.07	0.02	0.15	0.00	0.09	0.52
Other Mobile	0.00	0.01	0.03	0.02	0.06	0.00	0.42	0.55
Miscellaneous Area Sources	0.37	0.00	0.00	0.00	0.00	0.00	0.03	0.40
Initial Conditions	0.04	0.11	0.05	0.01	0.04	0.00	0.06	0.32
Boundary Conditions	0.23	1.21	0.30	0.07	0.25	0.01	0.34	2.41
Sum	0.86	2.67	0.82	0.30	1.12	0.18	1.52	7.47

EC: Elemental Carbon; POA: Primary Organic Aerosol; SOA: Secondary Organic Aerosol; OIN: Other Inorganics

Table 6. *Domainwide monthly-mean absolute ($\mu g\ m^{-3}$) contributions to the concentrations of $PM_{2.5}$ and its components in July from CAMx/PSAT*

Source	NH_4^+	SO_4^{2-}	NO_3^-	EC	POA	SOA	OIN	$PM_{2.5}$
Coal Combustion	0.00	1.58	0.00	0.00	0.00	0.00	0.05	1.64
Diesel Vehicles	0.00	0.04	0.01	0.09	0.03	0.00	0.00	0.17
Biomass Burning	0.01	0.01	0.00	0.02	0.10	0.00	0.06	0.21
Gasoline Vehicles	0.06	0.03	0.01	0.00	0.02	0.00	0.01	0.14
Industrial Processes	0.03	0.20	0.00	0.00	0.04	0.00	0.21	0.48
Waste Disposal and Treatment	0.00	0.00	0.00	0.00	0.01	0.00	0.01	0.03
Biogenic	0.01	0.00	0.00	0.00	0.00	0.33	0.01	0.35
Other Combustion	0.00	0.25	0.00	0.00	0.04	0.00	0.02	0.33
Other Mobile	0.00	0.03	0.00	0.03	0.04	0.00	0.33	0.43
Miscellaneous Area Sources	0.43	0.00	0.00	0.00	0.01	0.00	0.19	0.63
Initial Conditions	0.03	0.30	0.00	0.01	0.02	0.00	0.03	0.40
Boundary Conditions	0.19	1.23	0.00	0.11	0.40	0.01	0.14	2.08
Sum	0.77	3.69	0.03	0.26	0.73	0.35	1.06	6.89

EC: Elemental Carbon; POA: Primary Organic Aerosol; SOA: Secondary Organic Aerosol; OIN: Other Inorganics

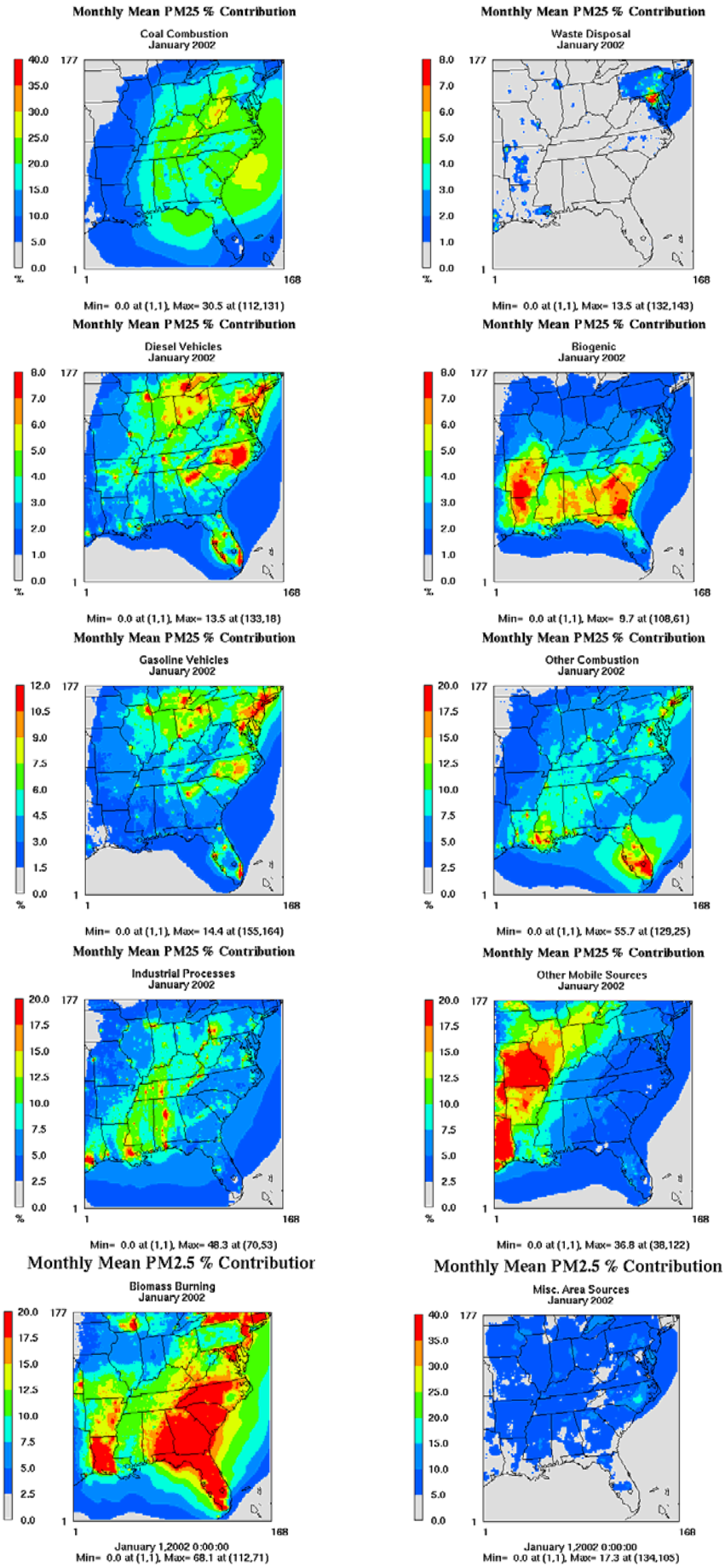

Figure 1. *Spatial distributions of monthly-mean percentage contributions to the concentrations of $PM_{2.5}$ from CAMx/PSAT in January.*

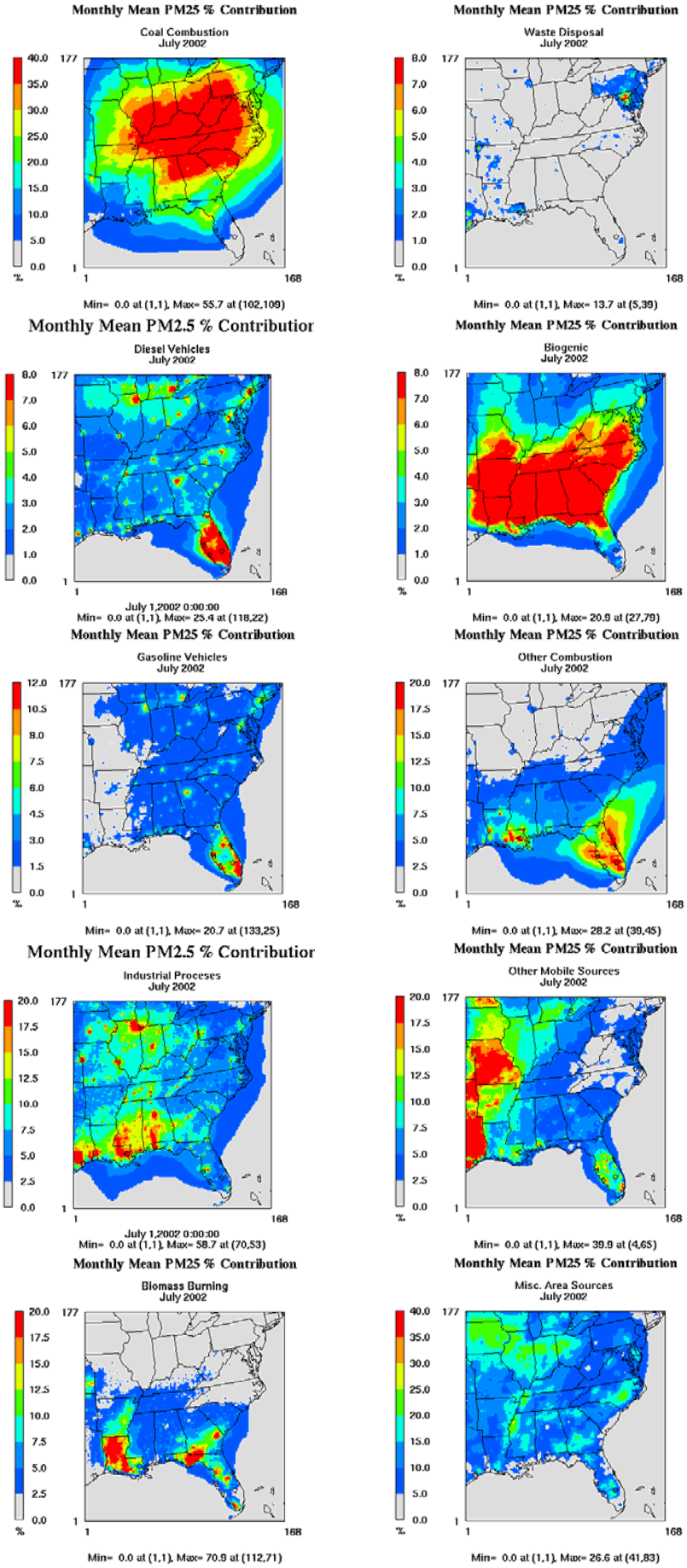

Figure 2. *Spatial distributions of monthly-mean percentage contributions to the concentrations of $PM_{2.5}$ from CAMx/PSAT in July.*

overall $PM_{2.5}$ contributions from these sources. Contributions from the two methods agree well for other combustion emissions in January, though CAMx/PSAT gives slightly higher contributions due to higher SO_4^{2-} contributions.

The largest discrepancies in contributions in January, both in terms of domain–averaged contributions and spatial distributions, occur for the miscellaneous area source category. The two methods agree that the largest contributions occur in regions where agricultural activities are high, particularly over eastern N.C. and throughout the upper Midwest. However, CMAQ/BFM tends to give much higher contributions in this region, nearly tripling overall $PM_{2.5}$ contributions from CAMx/PSAT in some areas. The large difference in overall $PM_{2.5}$ contributions is due to differences in contributions to NO_3^-. CMAQ/BFM gives a domainwide contribution of 7.5% (0.6 μg m^{-3}) to NO_3^- from miscellaneous area sources while CAMx/PSAT gives 0% contribution to NO_3^- across the entire domain. As discussed in Part I, this is due to the indirect effect captured by CMAQ/BFM in which NO_3^- can be formed when NH_4^+ is available. However, in CAMx/PSAT, each species is linked only to its direct primary precursor (e.g., $NO_x \rightarrow NO_3^-$, $SO_2 \rightarrow SO_4^{2-}$, $NH_3 \rightarrow NH_4^+$) (i.e., direct effect) and the impact of non–direct emission precursors (e.g., NH_3 emissions can affect the formation of SO_4^{2-} and NO_3^-) is not considered. In this case, NO_3^- is linked only to NO_x emissions, and is thus unaffected by NH_3 emissions from miscellaneous area sources in the CAMx/PSAT simulation. As discussed in several studies (e.g., Ansari and Pandis, 1998; Pun et al., 2008; and Zhang et al., 2009), non–linear indirect effects occur between secondary PM component (i.e., sulfate, nitrate, and organics) and their non–direct emission precursors. The omission of such indirect effects in the current formulation of CAMx/PSAT will limit its use for SA of secondary PM species.

CAMx/PSAT tends to give higher contributions to overall $PM_{2.5}$ from coal combustion emissions than does CMAQ/BFM in January. Coal combustion contributions to SO_4^{2-}, NO_3^-, POA, and SOA in January and July are shown in Figures 3 and 4, respectively. The largest difference in domainwide contributions between the two methods in January occurs for NH_4^+ (see Figure 5), NO_3^-, and SO_4^{2-} (see Figures 4 and 5 in Part I, Figures 3 and 4 in this paper). CMAQ/BFM gives higher contributions to NH_4^+ while CAMx/PSAT gives larger contributions to NO_3^- and SO_4^{2-}. The larger contributions to NH_4^+ from CMAQ/BFM are attributed to the indirect effects of SO_4^{2-} reductions on NH_4^+. Reductions in SO_2 emissions from coal combustion sources within the CMAQ/BFM lead to less formation of ammonium sulfate [$(NH_4)_2SO_4$], resulting in reductions in NH_4^+. However, because NH_4^+ is assumed to be affected only by NH_3 emissions in CAMx/PSAT, CAMx/PSAT gives relatively insignificant contributions to NH_4^+ from coal combustion emissions. As described in Part I, reductions in SO_2 emissions from coal combustion leave more oxidants and radicals available to oxidize NO_2, leading to net increases in NO_3^- in some areas by CMAQ/BFM. As shown in Figure 3 in this paper and Figure 4 in Part I, this indirect effect is not considered within CAMx/PSAT, thus leading to larger NO_3^- contributions from CAMx/PSAT. Figure 3 also shows that CAMx/PSAT tends to give higher SO_4^{2-} contributions than CMAQ/BFM in January. This difference in SO_4^{2-} contributions may be attributed to oxidant–limiting effects accounted for in CMAQ/BFM but not in CAMx/PSAT in which reductions in emissions of SO_2 from coal combustion sources in CMAQ/BFM leave more oxidants and radicals available to oxidize VOCs, NO_x, and SO_2 from other sources that compete for limited oxidants and radicals leading to smaller overall SO_4^{2-} contributions from CMAQ/BFM. Additionally, differences in wet deposition between CMAQ and CAMx may partially explain larger contributions from CAMx/PSAT, with CMAQ giving higher wet deposition of SO_4^{2-} in January, also leading to smaller contributions than those from CAMx/PSAT.

The spatial distributions of diesel vehicle $PM_{2.5}$ contributions to $PM_{2.5}$ concentrations agree fairly well between CAMx/PSAT and CMAQ/BFM, with the largest impacts occurring in the large urban areas of the domain (e.g., Chicago, NYC, Atlanta, Detroit, Cleveland, Miami, etc.). However, CAMx/PSAT gives higher $PM_{2.5}$ contributions than CMAQ/BFM over the majority of the domain. This is again attributed primarily to the interactions between NH_4^+, NO_3^-, and SO_4^{2-}, as contributions to primary species (OIN, EC, and POA) are nearly equivalent between the two methods. CAMx/PSAT tends to give higher contributions to NO_3^- than CMAQ/BFM in January (see Figure 7, Table 6 in Part I and Figure 6, Table 3 in Part II). Koo et al. (2009) found that CAMx/PSAT generally tends to predict higher NO_3^- contributions than CAMx/BFM due to NO_3^- formation being limited by availability of NH_4^+ in CAMx/BFM. The reductions in NO_3^- in CMAQ/BFM lead to reductions in NH_4^+ that follow a nearly identical spatial distribution at the NO_3^- reductions, due to indirect effects previously described. CAMx/PSAT also gives higher SO_4^{2-} contributions due to the indirect effects of NO_x emissions reductions on SO_4^{2-} within CMAQ/BFM, which lead to increases in SO_4^{2-} across much of the domain in the CMAQ/BFM due to increased availability of oxidants. Additionally, reductions in NO_x emissions from gasoline vehicles within the CMAQ/BFM will lead to reductions in HNO_3 that will reduce the acidity of the aqueous phase solution, allowing for increases in SO_4^{2-} in the aqueous phase.

As opposed to diesel vehicle contributions to $PM_{2.5}$ that are higher by CAMx/PSAT than CMAQ/BFM in January, $PM_{2.5}$ contributions from gasoline vehicles by CMAQ/BFM are higher than CAMx/PSAT. CMAQ/BFM gives higher NO_3^- contributions from gasoline vehicles than CAMx/PSAT (see Figure 7, and Table 6 in Part I and Figure 6, and Table 3 in Part II). This is due to higher NH_3 emissions from gasoline vehicles relative to diesel vehicles. Therefore, larger NH_4^- reductions from gasoline vehicle emissions further enhance NO_3^- reductions in CMAQ/BFM due to aforementioned indirect effects. This is the primary factor leading to higher overall $PM_{2.5}$ contributions from gasoline vehicles by CMAQ/BFM. CAMx/PSAT gives higher SO_4^{2-} contributions than CMAQ/BFM due to the indirect effects of reduction of NO_x emissions from diesel vehicles on SO_4^{2-} in CMAQ/BFM.

Both CAMx/PSAT and CMAQ/BFM agree well on the spatial distribution of biogenic contributions to $PM_{2.5}$ in January, with the largest impacts occurring over the Gulf States. CAMx/PSAT and CMAQ/BFM do, however, give different magnitudes of biogenic contributions to $PM_{2.5}$, due primarily to different SOA contributions from biogenic emissions. CMAQ/BFM tends to give higher contributions to SOA from biogenic emissions than CAMx/PSAT (2.7% vs. 1.9%) (See Table 6 in Part I and Table 3 in Part II). As shown in Figure 7, the CMAQ baseline simulation gives higher SOA concentrations than the CAMx simulation in January. Therefore, the difference in biogenic contributions to SOA in January is likely due to differences in simulated SOA concentrations between the two models. The other main difference between contributions from the two methods is the contributions of biogenic emissions to NO_3^-, with CMAQ/BFM giving a larger contribution than CAMx/PSAT. The NO_3^- contributions from CMAQ/BFM can be attributed to the indirect effect of NH_4^+ reductions on NO_3^-. As discussed, CAMx/PSAT assumes that NO_3^- is linked only to its primary precursor (i.e., NO_x), and is therefore unaffected by NH_3 emissions.

In July, CMAQ/BFM and CAMx/PSAT agree very well on the contributions to $PM_{2.5}$ from biomass burning, industrial processes, waste disposal and treatment, and other mobile sources. Emissions from these source categories are dominated by primary PM species, and thus, the two methods are expected to give similar contributions. The two methods also agree well on the contributions from gasoline vehicles, though CMAQ/BFM gives slightly higher contributions to SO_4^{2-} and NO_3^- due to the indirect

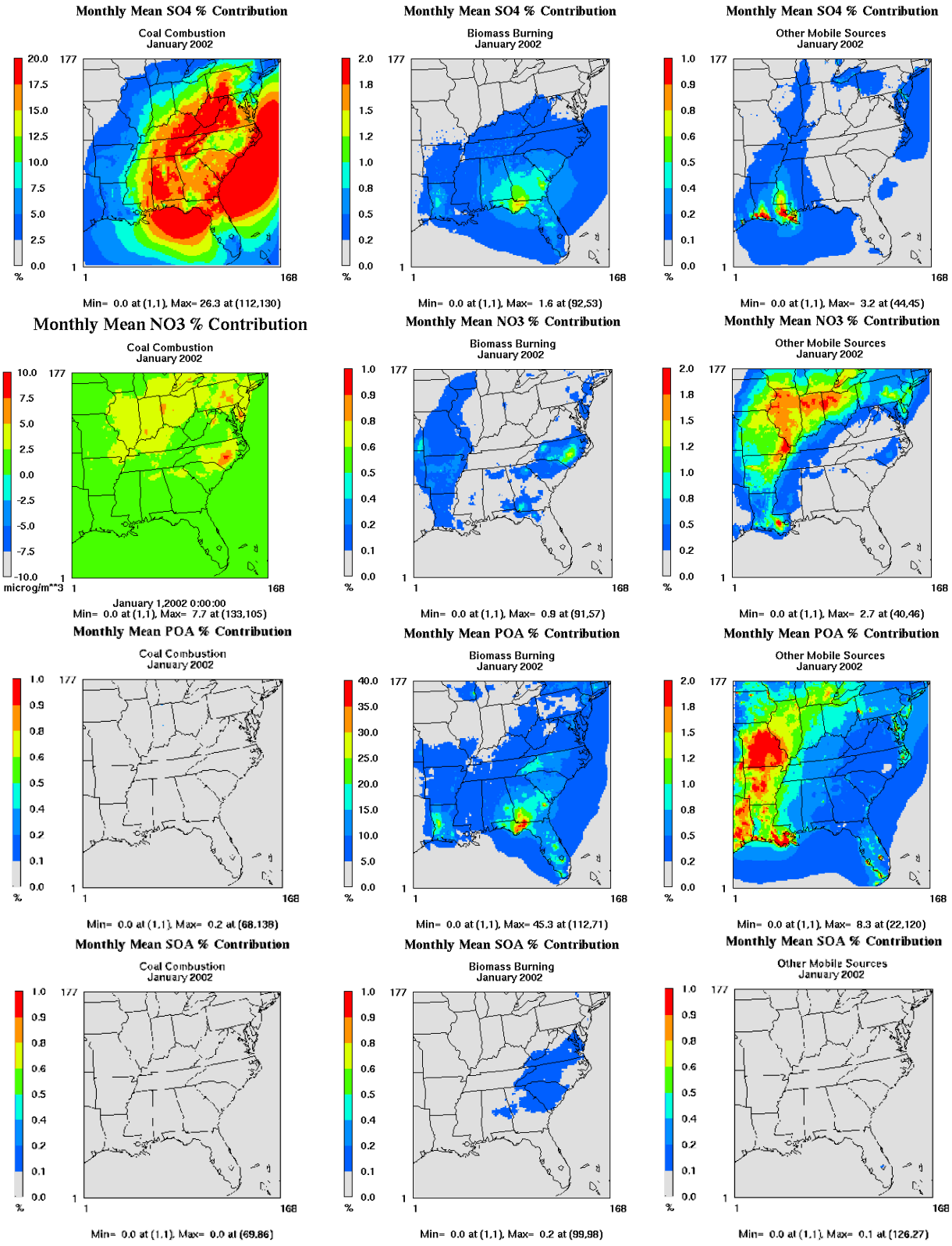

Figure 3. *Contributions of top three source categories (i.e., coal combustion, biomass burning, and other mobile sources) to the concentrations of SO_4^{2-}, NO_3^-, POA, and SOA in January from CAMx/PSAT.*

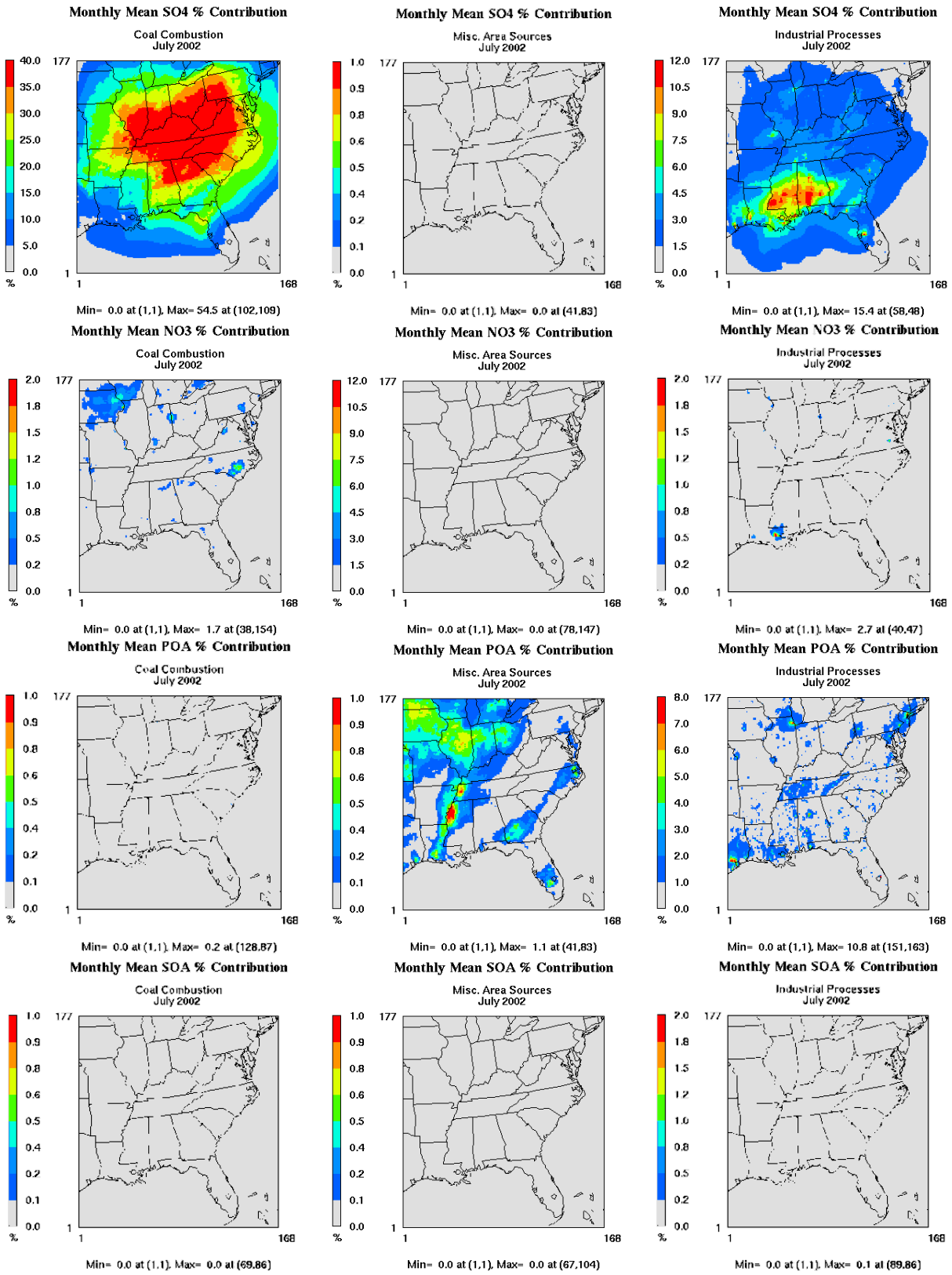

Figure 4. *Contributions of top three source categories (i.e., coal combustion, miscellaneous area sources, and industrial processes) to the concentrations of SO_4^{2-}, NO_3^-, POA, and SOA in July from CAMx/PSAT.*

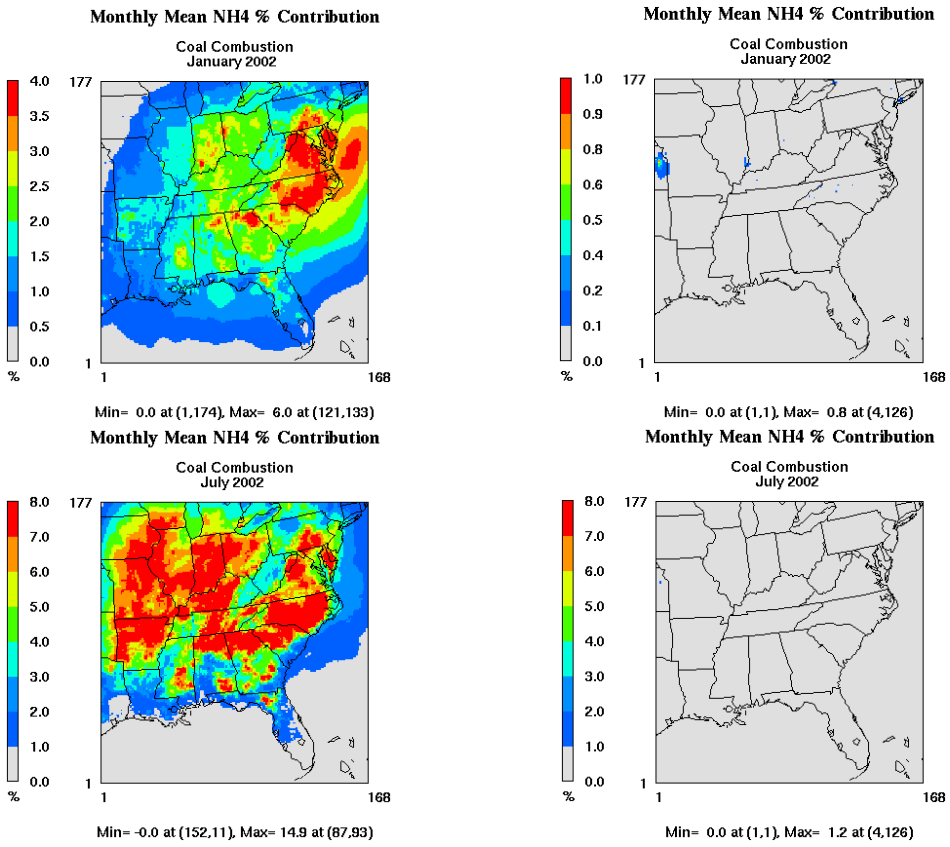

Figure 5. *Monthly-mean percentage contribution of coal combustion emissions to the concentrations of NH_4^+ from CMAQ/BFM (left) and CAMx/PSAT (right) in January (top) and July (bottom).*

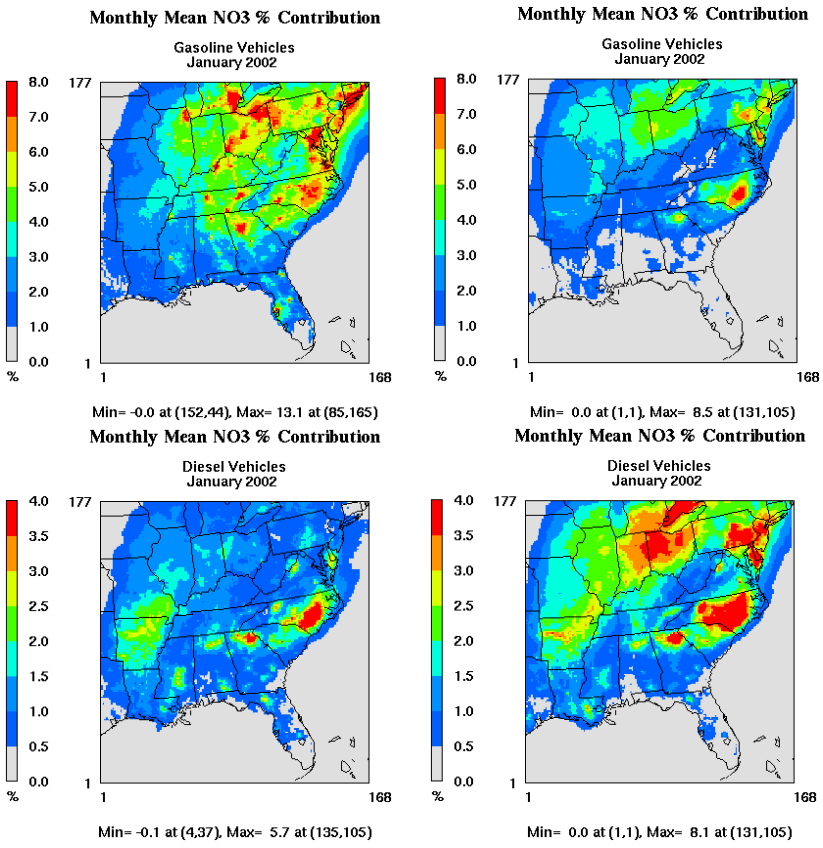

Figure 6. *Monthly-mean percentage contribution of gasoline vehicle emissions (top) and diesel vehicle emissions (bottom) to the concentrations of NO_3^- from CMAQ/BFM (left) and CAMx/PSAT (right) in January.*

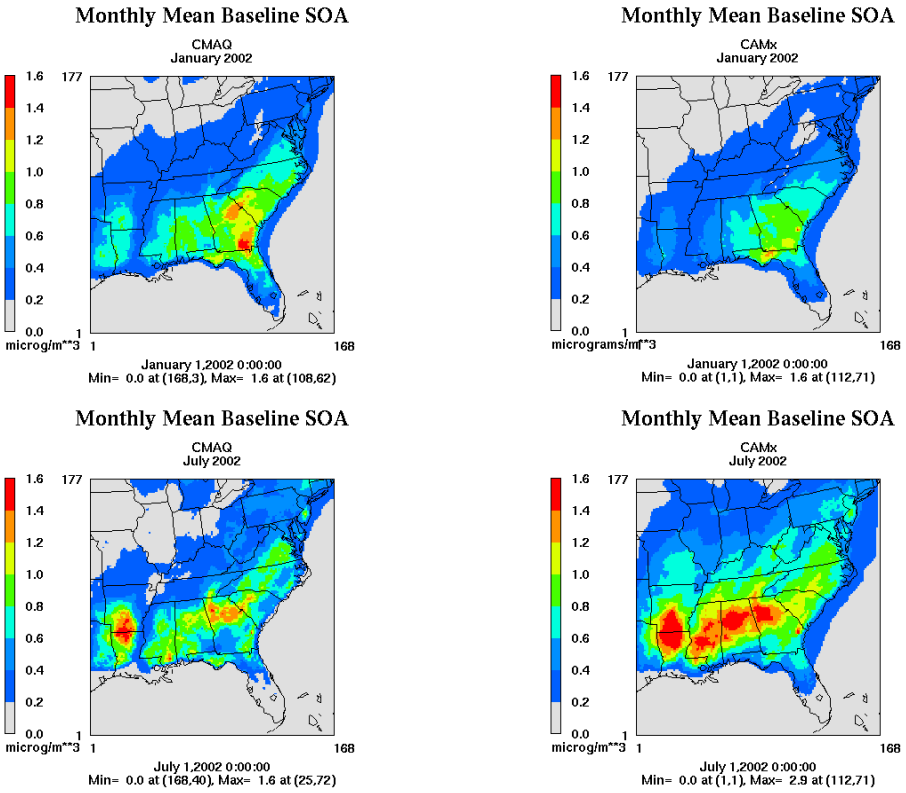

Figure 7. *Monthly-mean baseline SOA concentrations from CMAQ (left) and CAMx (right) in January (top) and July (bottom).*

effects of NH_4^+ reductions. The two methods are in better agreement on the contributions from miscellaneous area sources in July than in January, as the indirect effect associated with NH_4^+ and NO_3^- is much less important due to much lower NO_3^- concentrations in summer.

The largest discrepancy between source contributions from CMAQ/BFM and CAMx/PSAT in July occurs for biogenic sources. Different from January, CAMx predicts higher baseline SOA concentrations than CMAQ in July, as shown in Figure 7. This leads to higher biogenic SOA contributions from CAMx/PSAT when compared to CMAQ/BFM (4.2% vs. 3.4%). The largest differences between the two methods are the effects of biogenic emissions on NH_4^+, NO_3^-, and SO_4^{2-}. Figure 8 shows contributions to these species from CAMx/PSAT (see Figure 10 in Part I for similar plots from CMAQ/BFM). CAMx/PSAT gives NH_4^+ contributions in July that are similar to that of January; however, contributions to NO_3^- and SO_4^{2-} are minimal. Conversely, CMAQ/BFM gives slight increases over most of the domain for all 3 species when eliminating biogenic emissions, with the largest increasing occurring for SO_4^{2-}. As discussed in part I, this is due to the indirect effect simulated by CMAQ/BFM, in which decreased VOC emissions leave more oxidants and radicals available to oxidize precursors for other secondary PM species such as SO_2, NO_x, and NH_3; this effect is enhanced in July due to higher biogenic VOC emissions in the summer months.

The difference in simulated SOA concentrations between CMAQ and CAMx in January and July may be due to several factors. As mentioned, CMAQ simulates higher SOA in January while CAMx simulates higher SOA in July. The concentrations of SOA precursors such as isoprene and terpenes simulated by CMAQ are higher than those by CAMx (Figures not shown), due to lower concentrations of oxidants (see Figure 9) and radicals as a result of a stronger vertical mixing. This should in turn lead to lower SOA formation from CMAQ than from CAMx. However, higher SOA from CMAQ is found in January, which can be attributed to two main factors. First, SOA formed from sesquiterpenes is simulated by CMAQ but not simulated by CAMx although the SOA modules include the formation pathways for SOA from sesquiterpenes in both models. This is because the VISTAS emission file does not include sesquiterpene emissions needed for CAMx simulations, whereas CMAQ estimates sesquiterpene emissions by scaling monoterpene emissions which are available from the VISTAS emission file (Morris et al., 2006). Second, parameters used in the respective SOA modules of CMAQ and CAMx are different. In particular, Morris et al. (2006) reported that CMAQ uses a value of 156 KJ mol^{-1} for the enthalpy of vaporization (ΔH) whereas CAMx uses values of 42 – 75.5 KJ mol^{-1}. The enthalpy of vaporization is a thermodynamic parameter that represents the volatility of SOA (Zhang et al., 2007). Napelenok et al. (2008) asserted that the value used by CMAQ may be too high and may lead to exaggerated night–time and wintertime SOA peaks, explaining why CMAQ might give higher SOA in winter than CAMx. Conversely, CAMx gives higher SOA concentrations than CMAQ in July. While differences in SOA precursor concentrations and the value of ΔH between the two models also exist in July that will lead to the same trend in SOA formation as January (i.e., higher SOA by CMAQ than CAMx), the increases in SOA are compensated by another factor, leading to a net SOA concentration that is lower by CAMx. Namely, CAMx simulates considerably higher O_3 and H_2O_2 than CMAQ in July (see Figure 9 and also Table 3 in Part I and Table 2 in Part II). Higher concentrations of oxidants species lead to a higher oxidation of VOCs in CAMx, ultimately resulting in higher SOA concentrations in CAMx than CMAQ in July.

CAMx/PSAT and CMAQ/BFM agree that the largest contributions from diesel vehicles in July occur in large urban areas; however, CMAQ/BFM tends to give higher overall contributions than CAMx/PSAT across most of the domain. In contrast to January, CMAQ/BFM tends to give higher diesel vehicle contributions to NO_3^- and SO_4^{2-} in July; this may be attributed to the indirect effects of NH_4^+ reductions on NO_3^- and SO_4^{2-}. Similar to January, the overall $PM_{2.5}$ contributions from CMAQ/BFM are enhanced due to the indirect effect of NO_3^- and SO_4^{2-} reductions on NH_4^+.

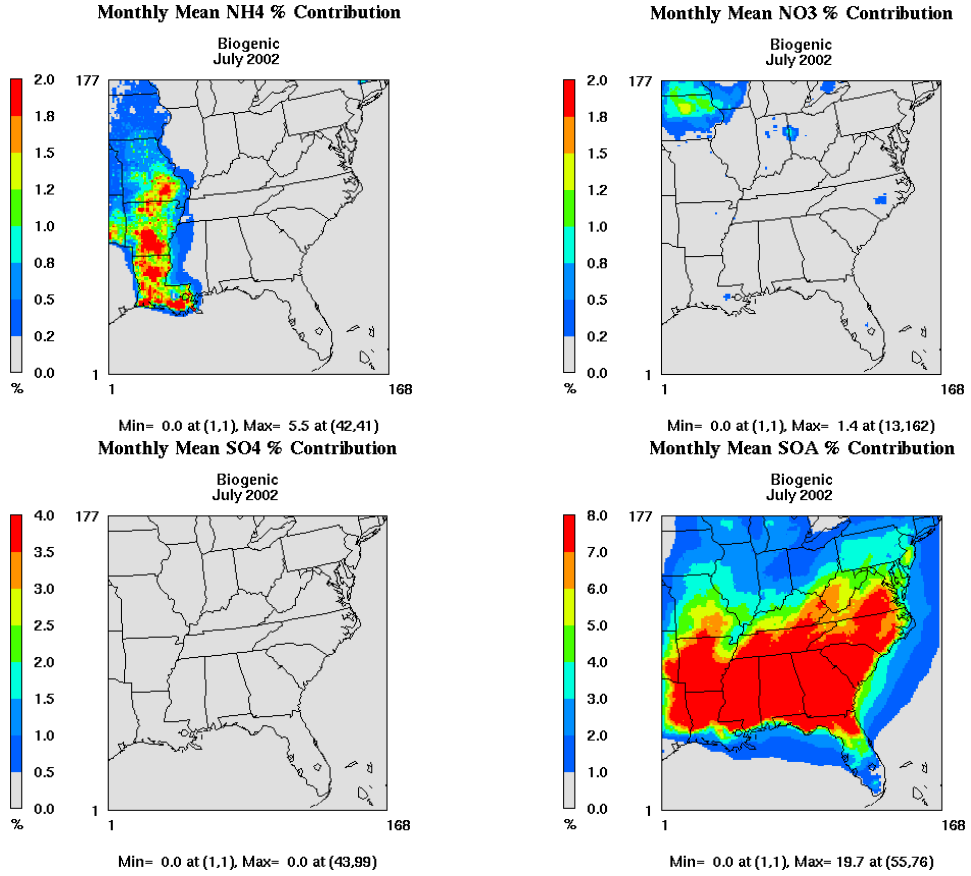

Figure 8. *Monthly mean percentage contributions to the concentrations of NH_4^+, NO_3^-, SO_4^{2-}, and SOA from biogenic emissions from CAMx/PSAT in July.*

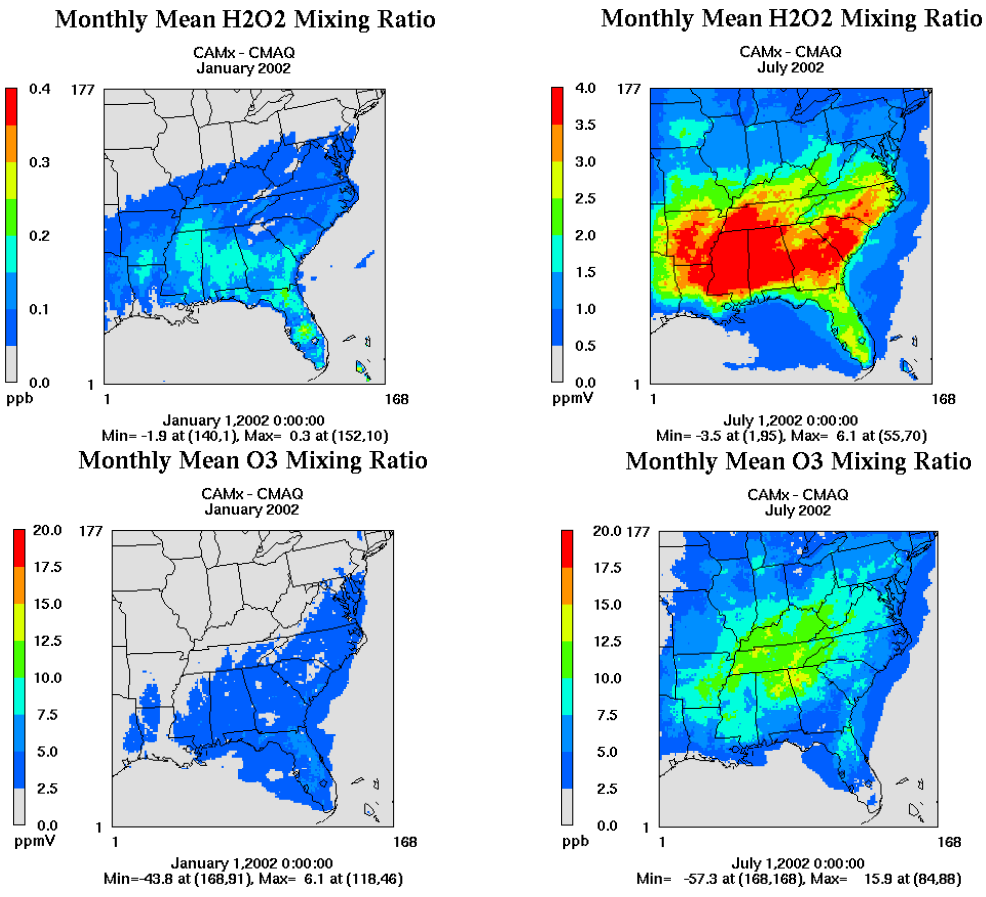

Figure 9. *Absolute difference in monthly-mean concentrations of H_2O_2 (top) and O_3 (bottom) between CAMx and CMAQ baseline simulations in January (top) and July (bottom).*

As opposed to January, CMAQ/BFM gives larger contributions to $PM_{2.5}$ from coal combustion than CAMx/PSAT in July. Domainwide contributions indicate that this difference is due to larger coal combustion contributions to NH_4^+ (see Figure 5) and SO_4^{2-} from CMAQ/BFM. The larger contributions to NH_4^+ are caused by indirect effects of SO_4^{2-} reductions on NH_4^+ that are not considered in CAMx/PSAT. Although CAMx predicts higher baseline H_2O_2 over the majority of the domain (see Figure 9) due to higher O_3 mixing ratios resulted from a weaker vertical mixing (this would lead to a positive effect on the source contribution to SO_4^{2-}), CAMx/PSAT actually gives slightly smaller contributions than CMAQ/BFM, as shown in Figure 4. Smaller contributions from CAMx/PSAT are attributed to differences in the wet deposition fluxes of SO_4^{2-} between CMAQ and CAMx. In July, CAMx gives considerably higher wet deposition fluxes of SO_4^{2-} than CMAQ over most of the domain except for Florida (see the SM, Figure S1) (this would lead to a negative effect on the source contribution to SO_4^{2-}), leading to smaller overall source contributions of CAMx/PSAT than CMAQ/BFM.

Other combustion contributions to $PM_{2.5}$ in July show a large difference between CMAQ/BFM and CAMx/PSAT over southern Florida. This is caused by a much larger contribution to SO_4^{2-} from CAMx/PSAT. Note that this is opposite to the trend for coal combustion over most of the domain where CAMx/PSAT gives lower source contributions from coal combustion to SO_4^{2-} than CMAQ/BFM. This can be attributed to two main factors. First, spatial distributions of SO_2 emissions from coal combustion and other combustion sources are different in Florida (i.e., SO_2 emissions from other combustion sources over Florida are comparable in magnitude to those in other states but there is no or little SO_2 emissions from coal combustion over Florida). Second, dominance of the aforementioned positive and negative effects on the source contributions of SO_4^{2-} may be different in Florida as compared to other states. Over Florida where the differences in the simulated wet deposition rate of SO_4^{2-} predicted from both models are smaller than over most of the domain, the positive effect due to a higher aqueous–phase oxidation rate of SO_2 dominates over the negative effect due to a higher wet deposition rate of SO_4^{2-} predicted from CAMx than CMAQ. The other main difference between CMAQ/BFM and CAMx/PSAT in July is a higher contribution to NH_4^+ from CMAQ/BFM resulting from indirect effects of NO_3^- and SO_4^{2-} reductions on NH_4^+.

While differences exist between the two methods in both months due to differences between CMAQ and CAMx, differences between the source apportionment methods appear to be larger during the winter months. One possible reason for the enhanced discrepancies during the winter months may be differences in meteorological conditions between January and July. As described previously, CMAQ and CAMx differ in their treatment of vertical mixing, with CAMx tending to give a weaker vertical mixing than CMAQ. As outlined by Olsen (2009), the Yamartino–Blackman Cubic advection option in CMAQ utilizes the Piecewise Parabolic Method (PPM) for horizontal advection. Air densities simulated by MM5 are then used to calculate the vertical velocities. Conversely, CAMx calculates vertical diffusion and advection implicitly. Such differences between CMAQ and CAMx result in a weaker vertical mixing by CAMx. This leads to larger differences between source contributions between the two models during the winter months when planetary boundary layer (PBL) heights are considerably lower. Perhaps even more important is the larger role of indirect effects associated with the $NH_4 - NO_3^- - SO_4^{2-}$ thermodynamic system during the winter months. Concentrations of NO_3^- are small during the summer months due to unfavorable meteorological conditions for formation, and thus, SO_4^{2-} is the dominant inorganic species and interactions between the species are not as important in July. However, during the winter months when NO_3^- concentrations are higher, these indirect effects resulting from the interactions of the $NH_4 - NO_3^- - SO_4^{2-}$ thermodynamic system become much more important.

4.3. Site specific analysis

Figure 10 shows source percentage contributions from both methods averaged at each of the 18 sites shown in Table 5 with similar characteristics (e.g., urban, rural, remote, and coastal). The largest differences between the two methods at urban sites in January occur for coal combustion and miscellaneous area source contributions. CAMx/PSAT gives larger contributions from coal combustion at urban sites [e.g., Pensacola (PNS), Cincinnati (CIN), Knoxville (KNX), and Nashville (NSH), see Table 7 for percentage contributions and Table 8 for corresponding absolute contributions], likely due to the indirect effects of SO_2 emissions reductions on NO_3^- in CMAQ/BFM. Conversely, CMAQ/BFM gives significantly higher contributions from miscellaneous area sources at most sites, with the largest difference for urban sites occurring at CIN [20.7% (2.5 μg m^{-3}) from CMAQ/BFM vs. 6.8% (1.0 μg m^{-3}) from CAMx/PSAT], due to the indirect effects of NH_4^+ reductions resulting from the elimination of miscellaneous area sources on NO_3^-. CMAQ/BFM also tends to give higher contributions from gasoline vehicles at urban sites in January, as reflected in contributions at Jefferson Street (Atlanta) (JST) (20.7% (3.9 μg m^{-3}) from CMAQ/BFM vs. 11.6% (2.4 μg m^{-3}) from CAMx/PSAT). This is attributed to the enhanced reductions of NH_4^- due to the indirect effects of NO_3^- reductions within CMAQ/BFM. Similarly, CMAQ/BFM gives larger contributions from biomass burning at urban sites in January, with the largest differences occurring at Charlotte (CLT) and New York City (NYC). This is attributed to larger contributions to NH_4^+ and NO_3^- within CMAQ/BFM that are a result of neglecting the interactions of these species in CAMx/PSAT. A similar pattern is observed for biogenic contributions at urban sites in January, with CMAQ/BFM giving slightly larger contributions than CAMx/PSAT. This may be attributed to higher SOA simulated within CMAQ in January due to the different SOA parameterizations within the two models previously discussed. Conversely, CAMx/PSAT gives slightly higher contributions from diesel vehicles at urban sites in January, as seen at CLT and NYC. Larger contributions from diesel vehicles from CAMx/PSAT are due to slightly larger contributions to NO_3^- at these sites. While diesel vehicle emissions are dominated by NO_x, they also contain a considerable amount of SO_2 (see Tables 4 and 5 in Part I). Therefore, smaller contributions from diesel vehicles at urban sites may be attributed to the indirect effects of SO_2 emissions reductions on NO_3^-. The results are more comparable at urban sites in July, though CMAQ/BFM gives considerably higher contributions from coal combustion at all urban sites, likely due to lower wet deposition in CMAQ and the indirect effects of SO_4^{2-} reductions on NH_4^+.

Results at rural sites in January show a similar pattern as urban sites, with CAMx/PSAT giving higher contributions from coal combustion and CMAQ/BFM giving higher contributions from miscellaneous area sources due to the aforementioned indirect effects within CMAQ/BFM. Differences in miscellaneous area source contributions are particularly high at Jamesville (JMS) [29.3% (3.6 μg m^{-3}) from CMAQ/BFM vs. 10.3% (1.2 μg m^{-3}) from CAMx/PSAT], a site known to have high agricultural NH_3 emissions. As expected, contributions from biogenic sources at rural sites are higher than at urban sites from both methods due to higher emissions of biogenic VOCs in these regions. CMAQ/BFM gives higher contributions from biogenic sources at rural sites in January in comparison to CAMx, likely due to its higher SOA concentrations. The difference in biogenic contributions between the two methods at rural in January is the largest at Centreville (CTR) (13.1% (1.0 μg m^{-3}) from CMAQ/BFM vs. 6.5% (0.6 μg m^{-3}) from CAMx/PSAT) and Oak Grove (OAK) (14.4% (0.8 μg m^{-3}) from CMAQ/BFM vs. 6.1% (0.4 μg m^{-3}) from CAMx/PSAT]. Results from the two models at rural sites are also more comparable in July,

Table 7. *Monthly-mean percentage contributions to the concentrations of $PM_{2.5}$ at representative sites in January from CAMx/PSAT (top 3 sources in bold)*

Site	Type	Biogenic		Biomass		Coal		Diesel		Gas		Industrial		Misc.		Other Comb		Other Mob		Waste		IC		BC		Leftover	
		Jan	Jul	Jan	Jul	Jan	Jul	Jan	Jul	Jan	Jul	Jan	Jul	Jan	Jul	Jan	Jul	Jan	Jul	Jan	Jul	Jan	Jul	Jan	Jul	Jan	Jul
JST	Urban	3.6	**9.7**	**17.8**	2.3	16	**37.8**	8.9	7.9	**11.6**	**9.3**	6.1	7.3	2.7	5.3	**14.2**	4.7	3.6	7.2	1.0	0.9	2.8	4.0	6.5	3.2	5.2	0.4
YRK	Rural	5.0	**11.6**	**19.3**	4.0	**19.6**	**41.5**	4.4	2.8	5.2	3.1	7.5	6.7	6.8	**11.5**	**8.8**	3.8	6.4	5.4	0.4	0.3	3.7	5.0	10.9	3.6	2.0	0.7
BHM	Urban	3.6	**8.9**	10.1	1.7	**13.1**	**24.0**	4.6	4.4	6.2	5.9	**31.9**	**36.4**	2.7	3.0	**13.0**	6.9	3.1	2.6	0.9	0.9	2.1	3.0	7.0	1.9	1.7	0.4
CTR	Rural	6.5	**17.2**	**15.4**	3.8	**21.1**	**32.4**	2.5	1.8	3.0	2.0	**12.1**	**12.9**	5.0	7.2	7.9	5.9	5.5	3.9	0.4	0.2	4.5	6.4	14.0	3.9	2.1	2.4
GFP	Urban	3.6	4.6	9.0	2.4	**14.9**	**16.1**	3.0	3.5	3.7	3.6	**10.5**	**14.4**	3.1	2.5	**11.6**	11.1	5.5	**12.8**	0.3	0.5	4.8	7.9	16.7	7.3	13.3	13.3
OAK	Rural	6.1	**12.0**	**10.0**	3.5	**20.7**	**21.5**	2.4	2.5	2.7	2.8	**10.3**	**13.8**	4.4	5.5	9.1	8.5	5.9	6.3	0.3	0.4	5.4	7.8	16.8	6.1	5.9	9.3
PNS	Urban	2.7	2.5	**12.9**	2.0	**17.9**	**21.5**	2.4	2.5	3.2	2.7	**13.9**	**10.5**	2.9	2.1	9.8	**6.4**	4.5	4.4	0.2	0.1	3.9	11.2	19.4	17.7	6.3	16.4
OLF	Rural	3.5	4.2	**19.6**	3.4	13.2	**17.2**	3.6	6.3	4.8	7.0	**15.1**	**19.6**	2.7	4.9	**14.6**	7.0	5.1	**8.6**	0.2	0.2	3.4	7.3	11.1	6.8	3.1	7.5
GRM	Park	2.7	**6.8**	**32.3**	1.3	**20.2**	**53.7**	3.0	2.5	3.3	2.8	**5.5**	5.9	4.1	**7.7**	5.0	2.5	3.3	1.9	0.3	0.3	4.1	6.8	15.3	7.1	0.9	0.7
CLT	Urban	3.5	**6.9**	**18.7**	1.5	**17.9**	**45.0**	8.4	5.2	**10.3**	6.1	6.1	5.8	4.0	**6.9**	9.5	3.5	3.3	6.5	1.6	1.4	3.0	3.9	7.4	6.9	6.3	0.4
JMS	Rural	4.1	**7.0**	**18.2**	1.6	**19.7**	**29.1**	5.3	2.9	6.3	2.2	6.2	5.5	**10.3**	**16.2**	7.5	3.7	3.4	2.4	0.9	0.6	3.7	6.3	12.1	19.2	2.3	3.3
CHI	Urban	1.0	2.1	6.0	0.2	6.8	**18.3**	8.2	**9.5**	**10.2**	6.9	**14.8**	**23.4**	2.6	6.6	**10.9**	4.3	10.2	7.1	4.2	3.6	1.0	2.1	23.9	14.9	0.2	1.0
NYC	Urban	0.8	2.4	**13.2**	0.2	**11.1**	**16.8**	8.8	**9.2**	11.0	7.1	9.3	**8.9**	5.7	6.0	**19.9**	6.4	4.3	3.3	1.5	1.3	1.1	3.0	12	34.3	1.3	1.1
NOR	Coastal	2.9	3.8	8.2	5.5	7.2	6.0	5.9	7.3	4.1	3.6	**14.7**	**24.4**	5.6	5.2	**18.6**	**18.9**	**8.9**	**10.5**	0.9	0.8	4.1	3.2	11.8	3.2	7.1	7.6
CIN	Urban	2.0	2.8	**10.0**	1.0	**18.8**	**46.1**	5.0	3.8	6.2	3.2	**9.6**	**9.7**	6.8	**9.9**	9.0	2.1	8.9	6.8	0.6	0.4	3.3	4.0	16.2	9.0	3.6	1.2
KNX	Urban	2.6	**6.5**	**12.8**	2.9	**15.8**	**36.2**	4.3	2.5	5.4	3.1	**30.9**	**27.5**	4.1	6.3	5.6	1.9	3.8	3.0	0.2	0.2	3.1	5.3	9.1	4.2	2.3	0.4
NFK	Coastal	2.5	4.0	**12.9**	0.7	**18.8**	**28.9**	4.6	3.6	8.0	5.1	7.4	**6.3**	4.8	5.8	**14.0**	5.1	3.6	**6.9**	1.4	0.9	3.1	4.2	10.4	24.4	8.5	4.1
NSH	Urban	2.6	7.0	**12.8**	4.0	**19.8**	**39.9**	6.3	4.8	6.0	3.8	**12.1**	**10.5**	6.6	**10.5**	9.7	3.2	6.2	4.1	0.4	0.2	3.6	5.7	13.2	5.4	0.7	0.9

JST: Jefferson Street (Atlanta), GA; YRK: Yorkville, GA; BHML Birmingham, AL; CTR: Centreville, AL; GFP: Gulfport, MS; OAK: Oak Grove, MS; PNS: Pensacola, FL; OLF: Outlying Landing, FL; GRM: Great Smoky Mountain National Park, TN; CLT: Charlotte, NC; JMS: Jamesville, NC; CHI: Chicago, IL; NYC: New York City, NY; NOR: New Orleans, LA; CIN: Cincinnati, OH; KNX: Knoxville, TN; NFK: Norfolk, VA; NSH: Nashville, TN

Table 8. *Monthly-mean absolute ($\mu g\ m^{-3}$) contributions to the concentrations of $PM_{2.5}$ at representative sites in January from CAMx/PSAT (top 3 sources in bold)*

Site	Type	Biogenic		Biomass		Coal		Diesel		Gas		Industrial		Misc.		Other Comb		Other Mob		Waste		IC		BC		Leftover	
		Jan	Jul	Jan	Jul	Jan	Jul	Jan	Jul	Jan	Jul	Jan	Jul	Jan	Jul	Jan	Jul	Jan	Jul	Jan	Jul	Jan	Jul	Jan	Jul	Jan	Jul
JST	Urban	0.8	**1.7**	**3.8**	0.4	3.4	**6.6**	1.9	1.4	**2.4**	**1.6**	1.3	1.3	0.6	0.9	**3.0**	0.8	0.8	1.3	0.2	0.2	0.6	0.7	1.4	0.6	1.1	0.1
YRK	Rural	0.5	**1.5**	**2.1**	0.5	**2.1**	**5.5**	0.5	0.4	0.6	0.4	0.8	0.9	0.7	**1.5**	**1.0**	0.5	0.7	0.7	0.0	0.0	0.4	0.7	1.2	0.5	0.2	0.1
BHM	Urban	0.6	**2.0**	1.8	0.4	**2.3**	**5.4**	0.8	1.0	1.1	1.3	**5.6**	**8.2**	0.5	0.7	**2.3**	1.5	0.5	0.6	0.2	0.2	0.4	0.7	1.2	0.4	0.3	0.1
CTR	Rural	0.6	**1.3**	**1.4**	0.3	**1.9**	**2.5**	0.2	0.1	0.3	0.2	**1.1**	**1.0**	0.4	0.6	0.7	0.5	0.5	0.3	0.0	0.0	0.4	0.5	1.2	0.3	0.2	0.2
GFP	Urban	0.3	0.3	0.7	0.1	**1.1**	**1.0**	0.2	0.2	0.3	0.2	**0.8**	**0.9**	0.2	0.1	**0.9**	0.7	0.4	**0.8**	0.0	0.0	0.4	0.5	1.2	0.4	1.0	0.8
OAK	Rural	0.4	**0.8**	**0.7**	0.2	**1.5**	**1.3**	0.2	0.2	0.2	0.2	**0.7**	**0.9**	0.3	0.3	0.7	0.5	0.4	0.4	0.0	0.0	0.4	0.5	1.2	0.4	0.4	0.6
PNS	Urban	0.2	0.1	**1.0**	0.1	**1.4**	**0.8**	0.2	0.1	0.3	0.1	**1.1**	**0.4**	0.2	0.1	0.8	**0.2**	0.4	0.2	0.0	0.0	0.3	0.4	1.5	0.7	0.5	0.6
OLF	Rural	0.4	0.2	**2.4**	0.2	1.6	**1.0**	0.4	0.4	0.6	0.4	**1.9**	**1.1**	0.3	0.3	**1.8**	0.4	0.6	**0.5**	0.0	0.0	0.4	0.4	1.4	0.4	0.4	0.4
GRM	Park	0.2	**0.6**	**2.0**	0.1	**1.2**	**4.9**	0.2	0.2	0.2	0.3	**0.3**	0.5	0.3	**0.7**	0.3	0.2	0.2	0.2	0.0	0.0	0.3	0.6	0.9	0.7	0.1	0.1
CLT	Urban	0.6	**1.1**	**3.0**	0.2	**2.9**	**7.1**	1.3	0.8	**1.6**	1.0	1.0	0.9	0.6	**1.1**	1.5	0.5	0.5	1.0	0.3	0.2	0.5	0.6	1.2	1.1	1.0	0.1
JMS	Rural	0.5	**0.6**	**2.1**	0.1	**2.2**	**2.5**	0.6	0.3	0.7	0.2	0.7	0.5	**1.2**	**1.4**	0.8	0.3	0.4	0.2	0.1	0.1	0.4	0.5	1.4	1.7	0.3	0.3
CHI	Urban	0.2	0.4	1.0	0.0	1.2	**3 .3**	1.4	**1.7**	**1.8**	1.2	**2.6**	**4.2**	0.5	1.2	**1.9**	0.8	1.8	1.3	0.7	0.6	0.2	0.4	4.2	2.7	0.0	0.2
NYC	Urban	0.2	0.5	**4.0**	0.0	**3.3**	**3.5**	2.6	1.9	**3.3**	1.5	2.8	**1.9**	1.7	1.3	**6.0**	1.3	1.3	0.7	0.5	0.3	0.3	0.6	3.6	7.2	0.4	0.2
NOR	Coastal	0.4	0.5	1.1	0.7	1.0	0.7	0.8	0.9	0.6	0.4	**2.0**	**3.0**	0.8	0.6	**2.6**	**2.3**	**1.2**	**1.3**	0.1	0.1	0.6	0.4	1.6	0.4	1.0	0.9
CIN	Urban	0.2	0.5	**1.2**	0.2	**2.3**	**8.7**	0.6	0.7	0.7	0.6	**1.2**	**1.8**	0.8	**1.9**	1.1	0.4	1.1	1.3	0.1	0.1	0.4	0.8	1.9	1.7	0.4	0.2
KNX	Urban	0.3	**1.1**	**1.7**	0.5	**2.1**	**6.2**	0.6	0.4	0.7	0.5	**4.0**	**4.7**	0.5	1.1	0.7	0.3	0.5	0.5	0.0	0.0	0.4	0.9	1.2	0.7	0.3	0.1
NFK	Coastal	0.3	0.5	**1.7**	0.1	**2.5**	**3.3**	0.6	0.4	1.0	0.6	1.0	**0.7**	0.6	0.7	**1.8**	0.6	0.5	**0.8**	0.2	0.1	0.4	0.5	1.4	2.8	1.1	0.5
NSH	Urban	0.3	0.9	**1.3**	0.5	**2.1**	**5.0**	0.7	0.6	0.6	0.5	**1.3**	**1.3**	0.7	**1.3**	1.0	0.4	0.6	0.5	0.0	0.0	0.4	0.7	1.4	0.7	0.1	0.1

JST: Jefferson Street (Atlanta), GA; YRK: Yorkville, GA; BHML Birmingham, AL; CTR: Centreville, AL; GFP: Gulfport, MS; OAK: Oak Grove, MS; PNS: Pensacola, FL; OLF: Outlying Landing, FL; GRM: Great Smoky Mountain National Park, TN; CLT: Charlotte, NC; JMS: Jamesville, NC; CHI: Chicago, IL; NYC: New York City, NY; NOR: New Orleans, LA; CIN: Cincinnati, OH; KNX: Knoxville, TN; NFK: Norfolk, VA; NSH: Nashville, TN

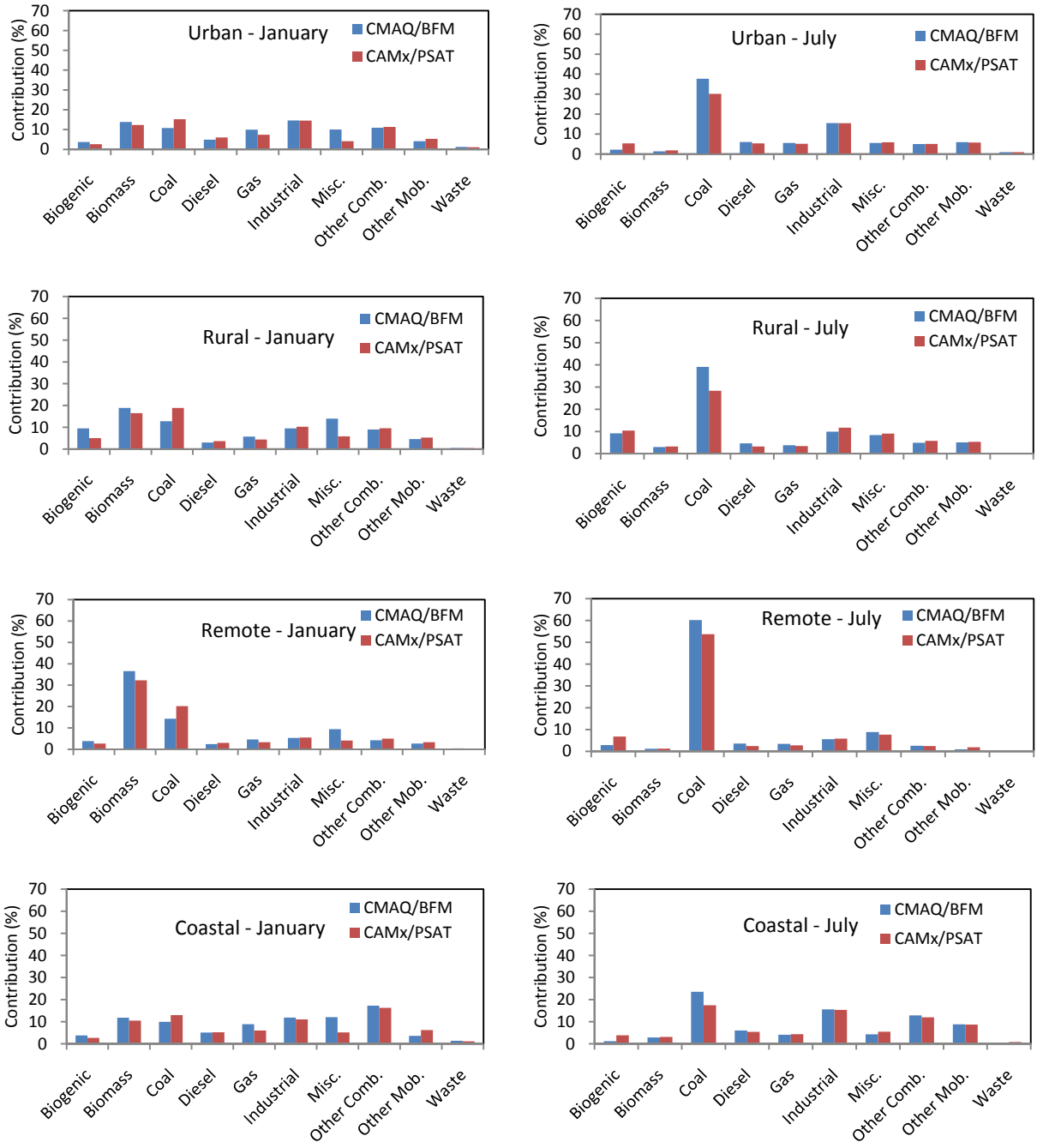

Figure 10. *Comparison of CAMx/PSAT and CMAQ/BFM monthly-mean percentage contributions to the concentrations of $PM_{2.5}$ at urban, rural, remote, and coastal sites in January (left) and July (right).*

with CMAQ/BFM giving larger contributions from coal combustion at all sites. Similar trends occur at remote sites in January, with CAMx/PSAT giving higher contributions from coal combustion and CMAQ/BFM giving higher contributions from miscellaneous area sources. CMAQ/BFM also gives higher contributions from biomass burning at remote sites in January, again likely due to higher contributions to NO_3^- and NH_4^+ resulting from indirect effects within CMAQ/BFM. In July the results are again more comparable, with CMAQ/BFM giving slightly higher contributions from coal combustion. The same trend is observed at coastal sites as well, with higher contributions to miscellaneous area sources and coal combustion from CMAQ/BFM in January and July, respectively, and higher contributions from coal combustion in January from CAMx/PSAT. Similar to other sites, CMAQ/BFM gives higher contributions from gasoline vehicles and biomass burning in January due the indirect effects previously described. CMAQ/BFM also gives higher contributions from biogenic sources at coastal sites in January for the same reason mentioned previously. Conversely, CAMx/PSAT gives higher contributions from other mobile sources at coastal sites in January. These higher contributions from other mobile sources are due primarily to higher contributions to SO_4^{2-}, likely due to higher H_2O_2 from CAMx (see Figure 9) leading to more aqueous–phase production of SO_4^{2-}.

Figure 11 shows a comparison of SA results at JST from this study with those from previous studies using various methods in January and July 2002. Sources most consistent with those examined in this study are chosen to ensure a fair comparison. Those sources include gasoline vehicles, diesel vehicles, industrial processes, biomass burning, and coal combustion. Additionally, studies conducting source apportionment for similar meteorological conditions are chosen whenever possible (i.e.,

January results from this study compared to results obtained from other studies during winter months). The results by Zheng et al. (2002) were obtained for January 2000 and July 1999 using chemical mass balance (CMB) with particle phase organic compounds as tracers. The results by Zheng et al. (2006) were obtained using molecular–maker based chemical mass balance modeling (CMB–MM). The January results from Zheng at al. (2006) were obtained by averaging results from December 11 and 17 of 2004 (denoted as W03 in Figures 11–12) and January 13, 16, and 22 of 2004 (denoted as W04 in Figures 11–12). Ke et al. (2008) results were obtained for July 2001 and January 2002 using positive matrix factorization (PMF) with five gaseous components (denoted as PMF1 in Figure 11) and eight thermal–resolved carbon fractions (denoted as PMF2 in Figure 11). The Lee et al. (2009) results were obtained for January 2002 and July 2002 using CMB–Lipschitz Generalized Optimization (LGO). Bhave et al. (2007) used CMAQ v4.4 instrumented to track primary EC and OC in July 1999. The studies used for comparison all only apportion the primary fraction of $PM_{2.5}$ mass to each source, with Bhave et al. (2007) only considering primary carbon species. The biggest discrepancy between results from this study and the receptor–oriented studies occurs for coal combustion in both January and July. This is due to the receptor–based studies limitation to primary PM species. Figure 11 also shows contributions from secondary sulfate and nitrate as resolved by the receptor–based studies. As shown, secondary SO_4^{2-} is a significant contributor, particularly in July. If we consider that a significant portion of this mass is likely due to coal combustion, the results from the receptor–based approaches and the source oriented methods in this study become more comparable. CMAQ/BFM and CAMx/PSAT agree well in differences in the importance of biomass burning between January and July, with larger contributions occurring in January. The contributions are comparable in magnitude, though differences between studies are expected due to larger temporal variations in biomass burning emissions. CMAQ/BFM gives higher contributions from gasoline motor vehicles in both months, again likely due to the exclusion of secondary species such as NO_3^- and SO_4^{2-} within the receptor–based approaches. CMAQ/BFM also gives higher contributions from gasoline motor vehicles than CAMx/PSAT due to the previously mentioned indirect effects. Source contributions from secondary nitrate may explain some of the differences in gasoline vehicle source contributions between the source–oriented methods and the receptor–based approaches. Contributions from diesel and gasoline vehicles are comparable among all the studies, though Zheng et al. (2002) gives significantly higher contributions than the other studies, likely due to differences in emissions for that particular episode. Diesel vehicle emissions are comprised more emissions of primary PM species (e.g., EC and POA) than those from gasoline vehicles, explaining the more comparable contributions for diesel vehicles than gasoline vehicles among studies.

Figure 12 shows a similar comparison of the CMAQ/BFM and CAMx/PSAT with receptor–based methods at CTR, a rural site, in both January and July. The approach of Zheng et al. (2002; 2006) and Bhave et al. (2007) are identical to that at JST. The contributions of gasoline vehicles from CMAQ/BFM and CAMx/PSAT are consistent with those of other studies, with contributions of less than 5% in both months. Coal combustion is not a resolved source in other studies at CTR in January, though estimates of secondary sulfate from the other studies are somewhat comparable to the coal combustion contribution from CMAQ/BFM and CAMx/PSAT. The contributions of biomass burning at CTR in January vary considerably among the studies, indicating a large variation in biomass burning emissions due to significant variations in burning activities. Similar to JST in January, Zheng et al. (2002) gives the highest contributions from diesel vehicles at CTR in January, indicating possible differences in meteorology (e.g., mixing heights and precipitation) and emissions for that particular episode. Industrial processes are not a resolved source from any of the studies at CTR in January, and thus no comparison can be made. The contributions from diesel vehicles in July are comparable among studies. Bhave et al. (2007) give higher contributions from biomass burning, while Zheng et al. (2002) and this study are comparable. Gasoline vehicles, industrial processes, and coal combustion are resolved only by Bhave et al. (2007) and this study. While contributions from gasoline vehicles are comparable, CMAQ/BFM and CAMx/PSAT give higher contributions from industrial processes and coal combustion, likely due to the limitation of Bhave et al. (2007) to primary carbon species.

4.4. Comparison of computational speeds of CMAQ/BFM and CAMx/PSAT

For a 1–month simulation consisting of 19 layers, a 1–month source apportionment simulation with CAMx/PSAT for 4 source categories using 6 processors required ~55.8 CPU hours. Conversely, a 1–month source apportionment simulation with CMAQ/BFM for 4 source category using 6 processors took ~210 hours to complete, making CAMx/PSAT nearly 4 times faster than CMAQ/BFM. Note that different aerosol size resolutions (2 bins in CAMx vs. 3 modes in CMAQ) may explain some of the differences in the CPU costs, in addition to differences in model treatments of major chemical and physical processes.

5. Conclusions

In this study, source apportionment results obtained using CAMx/PSAT are contrasted with those from the CMAQ/BFM described in Part I. Model evaluation shows that CAMx overpredicts max 1– and 8–h O_3 at all sites in both January and July, with the largest biases occurring at the AIRS–AQS sites in January and at the SEARCH sites in July. 24–hr average $PM_{2.5}$ is overpredicted at all networks in January, with the worst performance occurring at the SEARCH sites. Conversely, $PM_{2.5}$ is underpredicted at all networks in July with the largest biases occurring for the IMPROVE sites. Relative to CAMx, CMAQ performs better for both max 1– and 8–h O_3 in both months; performance for 24–h average $PM_{2.5}$ is comparable between the models. The models performance in terms of individual PM components is overall comparable at most sites, though CAMx performs slightly better in simulating organic carbon in both months. Additionally, CMAQ performs much better in simulating the wet deposition fluxes of NO_3^-, SO_4^{2-}, and NH_4^+ in both months.

CAMx/PSAT gives coal combustion, biomass burning, and other mobile sources as the three most important sources of $PM_{2.5}$ domainwide in January, differing from CMAQ/BFM that gives biomass burning, miscellaneous area sources, and coal combustion as the top three sources domainwide. The two methods agree that the top three contributors in July are coal combustion, miscellaneous area sources, and industrial processes, though they differ considerably in the magnitude of contributions from coal combustion.

The largest cause of discrepancy between CAMx/PSAT and CMAQ/BFM occurs due to the interactions of secondary species within CMAQ/BFM. Reductions in the emissions of precursors for secondary PM species (e.g., SO_2, NO_x, and NH_3) within the CMAQ/BFM can indirectly affect the formation of other secondary PM species. Differences between the two methods appear to be enhanced in January, possibly due to the increased importance of interactions within the $NH_4^+ – NO_3^- – SO_4^{2-}$ system in winter when NO_3^- is a more significant PM component and also the oxidant limiting effect in January when the concentrations of oxidant and radical species are lower. For primary PM species, the contributions from CMAQ/BFM and CAMx/PSAT are very similar, as the concentrations of these species are linearly related to emissions. Therefore, differences in contributions to primary PM species between the two methods can be mainly attributed to differences in the underlying models rather than difference in source apportionment methods.

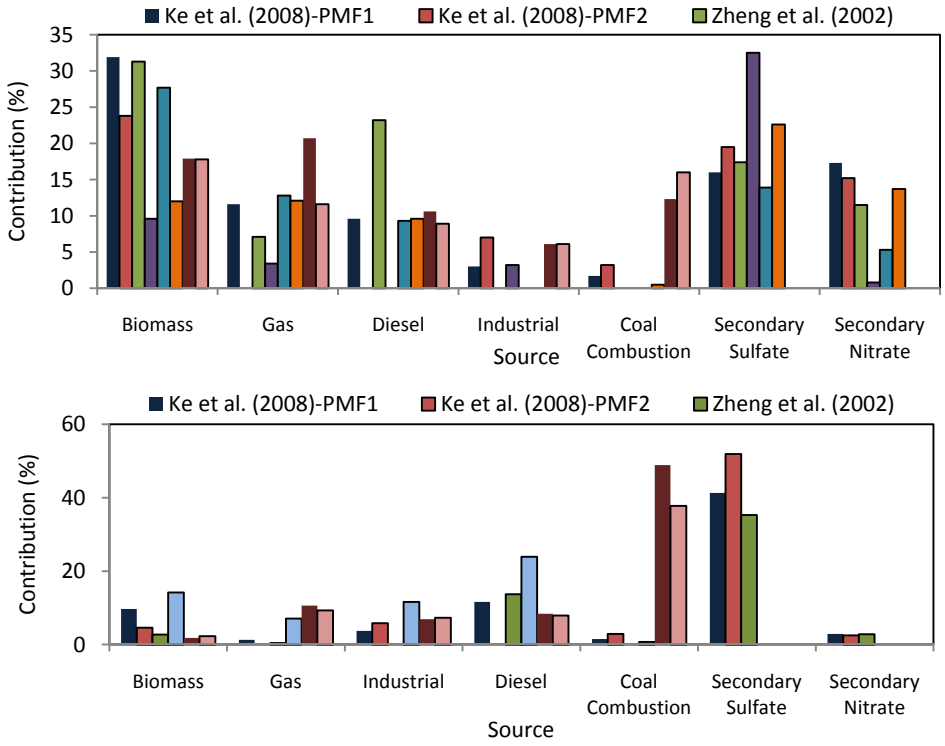

Figure 11. *Comparison of SA results with CMAQ/BFM, CAMx/PSAT, and other methods at JST in January (top) and July (bottom). Ke et al. (2008)-PFM1 and Ke et al. (2008)-PFM2 denote PMF with five gaseous components and 8 thermal-resolved carbon fractions, respectively and Zheng et al. (2006)-W03 and Zheng et al. (2006)-W04 denote results from December 2003 and January 2004, respectively.*

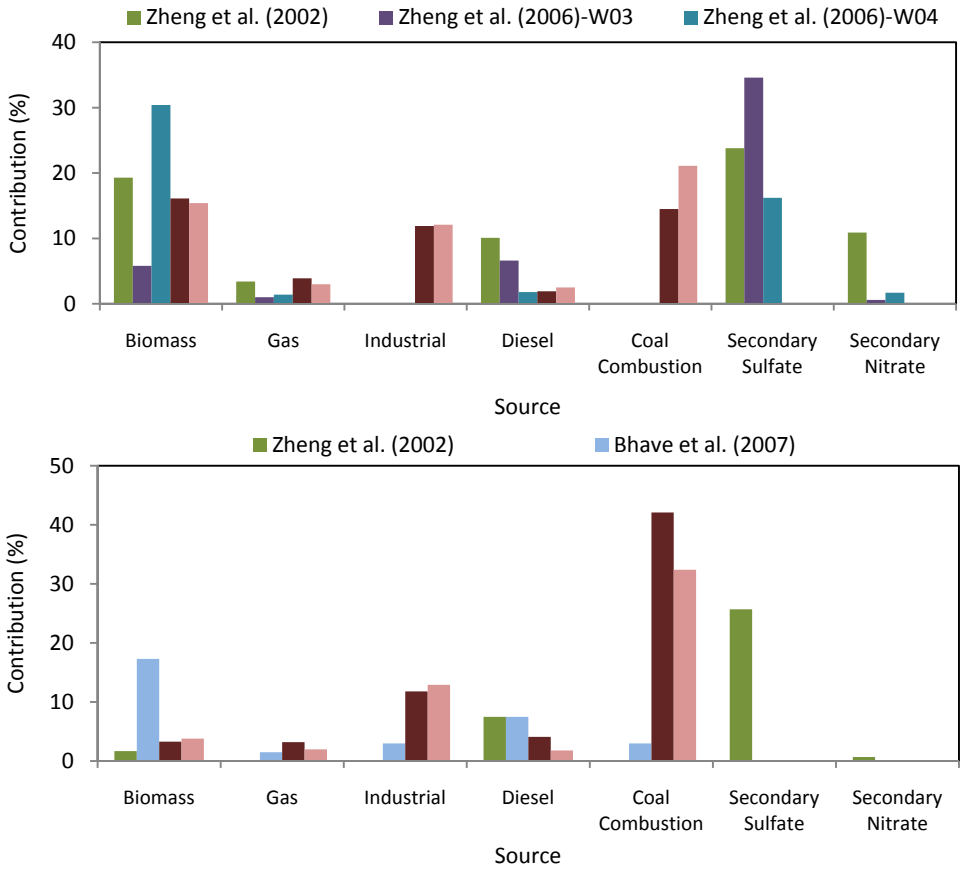

Figure 12. *Comparison of SS and SA results with other studies at CTR in January (top) and July (bottom). Zheng et al. (2006)-W03 and Zheng et al. (2006)-W04 denote results from December 2003 and January 2004, respectively.*

The results of this study indicate that CAMx/PSAT and CMAQ/BFM will give different SA results with different implications, particularly for winter episodes when nitrate concentrations are high. The CMAQ/BFM is feasible in analyzing emission reduction scenarios for both primary and secondary PM species as it captures the indirect effects that occur as a result of the interactions of pollutants in the atmosphere. Its limitation for secondary PM is associated with the fixed extent of the perturbation used. However, SS simulated with the CMAQ/BFM is different from "source apportionment", as the summation of the contributions of all source categories will not always equal the total $PM_{2.5}$ concentration. While CAMx/PSAT fails to capture indirect effects that are part of the present–day atmosphere (e.g., NO_3^- formation is limited by the availability of NH_4^+), it is able to apportion well each PM species to its primary emission precursor when indirect effects are insignificant and can provide accurate SA for primary PM species, with less computational demands than CMAQ/BFM. However, the use of CAMx/PSAT source apportionment data for exposure analysis will over– or under–estimate exposure to certain species due to the exclusion of indirect effects and oxidant–limiting effects that occur in the atmosphere. Both methods are shown to be subject to their own inherent limitations, and each should be used cautiously and accordingly in support of SIP modeling and epidemiological studies. One possible alternative, as shown by Lee et al. (2009), is to use an ensemble approach that considers source apportionment results for a particular source category from several different source apportionment methods. None of these current methods, however, can provide accurate SA for a system in which the relationship between precursor emissions and all secondary PM components is highly non–linear.

Acknowledgements

This work is supported by the U.S. EPA's Science to Achieve Results (STAR) grant #R833633 and the USDA National Research Initiative Competitive Grant no. 2008–35112–18758. We would also like to thank Alpine Geophysics, Inc. and the North Carolina Division of Air Quality for providing the emissions inventory and baseline simulation data of which the source apportionment results in this study are based on. Additional thanks are owed to Gary Wilson, Ralph Morris, and Greg Yarwood at ENVIRON, Inc. for their guidance in setting up the CAMx/PSAT simulations.

Supporting Material Available

CAMx Model Evaluation and Comparison with CMAQ; Monthly–mean absolute difference in the wet deposition fluxes of NH_4^+, NO_3^-, and SO_4^{2-} from CMAQ and CAMx (i.e., CAMx – CMAQ) in January and July (Figure S1); Spatial distribution monthly–mean concentrations of max 8–hr O_3 (top) and 24–hr average $PM_{2.5}$ simulated by CAMx overlaid with observations from AIRS–AQS, IMPROVE, STN, and SEARCH in January and July (Figure S2); Performance statistics for surface concentrations of $PM_{2.5}$ components simulated by CAMx in January 2002 (Table S1); Performance statistics for surface concentrations of $PM_{2.5}$ components simulated by CAMx in July 2002 (Table S2.).This information is available free of charge via the Internet at http://www.atmospolres.com.

References

Ansari, A.S., Pandis, S.N., 1998. Response of inorganic PM to precursor concentrations. *Environmental Science and Technology* 32, 2706-2714.

Baek, J., Park, S.K., Hu, Y., Russell A.G., 2005. Source apportionment of fine organic aerosol using CMAQ Tracers. *Proceedings of the Models-3 User's Workshop*, July 27, 2005. Research Triangle Park, North Carolina.

Bhave, P.V., Pouliot, G.A., Zheng, M., 2007. Diagnostic model evaluation for carbonaceous $PM_{2.5}$ using organic markers measured in the southeastern US. *Environmental Science and Technology* 41, 1577-1583.

Burr, M., Zhang, Y., 2011. Source apportionment of fine particulate matter over the Eastern U.S. Part I: source sensitivity simulations using CMAQ with the Brute Force method. *Atmospheric Pollution Research* 2, 299-316.

Byun, D., Schere, K.L., 2006. Review of the governing equations, computational algorithms, and other components of the models-3 Community Multiscale Air Quality (CMAQ) modeling system. *Applied Mechanics Reviews* 59, 51-77.

Cohan, D.S., Hakami, A., Hu, Y.T., Russell, A.G., 2005. Nonlinear response of ozone to emissions: source apportionment and sensitivity analysis. *Environmental Science and Technology* 39, 6739-6748.

Dunker, A.M., Yarwood, G., Ortmann, J.P., Wilson, G.M., 2002. Comparison of source apportionment and source sensitivity of ozone in a three-dimensional air quality model. *Environmental Science and Technology* 36, 2953-2964.

ENVIRON, 2009. Comprehensive Air Quality Model with Extensions (CAMx), Version 5.10. User's Guide,ENIRON International Corporation, Navato, CA, available at: http://www.camx.com.

Ke, L., Liu, W., Wang, Y., Russell, A.G., Edgerton, E.S., Zheng M., 2008. Comparison of PM2.5 source apportionment using positive matrix factorization and molecular marker-based chemical mass balance. *Science of the Total Environment* 394, 290-302.

Koo, B., Wilson, G.M., Morris, R.E., Dunker, A.M., Yarwood, G., 2009. Comparison of source apportionment and sensitivity analysis in a particulate matter air quality model. *Environmental Science and Technology* 43, 6669-6675.

Lee, D., Balachandran, S., Pachon, J., Shankaran, R., Lee, S., Mulholland, J.A., Russell, A.G., 2009. Ensemble-trained $PM_{2.5}$ source apportionment approach for health studies. *Environmental Science and Technology* 43, 7023-7031.

Morris, R.E., Koo, B., Guenther, A., Yarwood, G., McNally, D., Tesche, T.W., Tonnesen, G., Boylan, J., Brewer, P., 2006. Model sensitivity evaluation for organic carbon using two multi-pollutant air quality models that simulate regional haze in the southeastern United States. *Atmospheric Environment* 40, 4960-4972.

Napelenok, S.L., Carlton A.G., Bhave, P.V., Sarwar, G., Pouliot, G., Pinder, R. W., Edney, E. O., Houyoux, M., Foley K.M., 2008. Updates to the treatment of secondary organic aerosol treatment in CMAQv4.7, *Proceedings of the 7th Annual CMAS Conference*, 6-8 October 2008, Chapel Hill, N.C.

Olsen, K., 2009. *Fine Scale Modeling of Agricultural Air Quality Over The Southeastern United Staets: ApplicationaAnd Evaluation of Two Air Quality Models*. MS Thesis, North Carolina State University, Raleigh, NC.

Pun, B.K., Seigneur, C., Bailey, E.M., Gautney, L.L., Douglas, S.G., Haney, J.L., Kumar, N., 2008. Response of atmospheric particulate matter to changes in precursor emissions: a comparison of three air quality models. *Environmental Science and Technology* 42, 831-837.

Wesley, M.L., 1989. Parameterization of surface resistances to gaseous dry deposition in regional scale numerical models. *Atmospheric Environment* 23, 1293-1304.

Zhang, Y., Wen, X.Y., Wang, K., Vijayaraghavan, K., Jacobson, M.Z., 2009. Probing into regional O_3 and particulate matter pollution in the United States Part II. an examination of formation mechanisms through a process analysis technique and sensitivity study. *Journal of Geophysical Research-Atmospheres* 114, art. no. D22305.

Zhang, Y., Huang, J.P., Henze, D.K., Seinfeld, J.H., 2007. Role of isoprene in secondary organic aerosol formation on a regional scale. *Journal of Geophysical Research-Atmospheres* 112, art. no. D20207.

Zhang, Y., Liu, P., Queen, A., Misenis, C., Pun, B., Seigneur, C., Wu, S.Y., 2006. A comprehensive performance evaluation of MM5-CMAQ for the Summer 1999 Southern Oxidants Study episode, Part II. gas and aerosol predictions. *Atmospheric Environment* 40, 4839-4855.

Zhang, Y., Vijayaraghavan, K., Seigneur, C., 2005. Evaluation of three probing techniques in a three-dimensional air quality model. *Journal of Geophysical Research-Atmospheres* 110, art. no. D02305.

Zheng, M., Ke, L., Edgerton, E.S., Schauer, J.J., Dong, M.Y., Russell, A.G., 2006. Spatial distribution of carbonaceous aerosol in the southeastern United States using molecular markers and carbon isotope data. *Journal of Geophysical Research-Atmospheres* 111, art. no. D10S06.

Zheng, M., Cass, G.R., Schauer, J.J., Edgerton, E.S., 2002. Source apportionment of $PM_{2.5}$ in the southeastern United States using solvent-extractable organic compounds as tracers. *Environmental Science and Technology* 36, 2361-2371.